Fisheries and Oceans Canada | Pêches et Océans Canada
Ecosystems and Oceans Science | Sciences des écosystèmes et des océans

Canadian Science Advisory Secretariat (CSAS)

Research Document 2025/006

Ontario and Prairie Region and Arctic Region

Beluga Whale (*Delphinapterus leucas*) Abundance Estimate from Aerial Surveys of the Eastern Beaufort Sea Population in 2019

Marianne Marcoux[1], Alexandra Mayette[1], Megan Ferguson[2], Claire A. Hornby[1], and Lisa L. Loseto[1]

[1] Freshwater Institute
Fisheries and Oceans Canada
501 University Crescent
Winnipeg, Manitoba, R3T 2N6

[2] Alaska Fisheries Science Center
National Oceanic and Atmospheric Administration
7600 Sand Point Way NE
Seattle, WA 98115 USA

May 2025

Canada

Foreword

This series documents the scientific basis for the evaluation of aquatic resources and ecosystems in Canada. As such, it addresses the issues of the day in the time frames required and the documents it contains are not intended as definitive statements on the subjects addressed but rather as progress reports on ongoing investigations.

Published by:

Fisheries and Oceans Canada
Canadian Science Advisory Secretariat
200 Kent Street
Ottawa ON K1A 0E6

http://www.dfo-mpo.gc.ca/csas-sccs/
csas-sccs@dfo-mpo.gc.ca

ISSN 1919-5044
ISBN 978-0-660-75329-4 Cat. No. Fs70-5/2025-006E-PDF

Correct citation for this publication:

Marcoux, M., Mayette, A., Ferguson, M., Hornby, C.A., and Loseto, L.L. 2025. Beluga Whale (*Delphinapterus leucas*) Abundance Estimate from Aerial Surveys of the Eastern Beaufort Sea Population in 2019. DFO Can. Sci. Advis. Sec. Res. Doc. 2025/006. iv + 41 p.

Aussi disponible en français :

*Marcoux, M., Mayette, A., Ferguson, M., Hornby C.A. et Loseto, L.L. 2025. Estimation de l'abondance des bélugas (*Delphinapterus leucas*) d'après les relevés aériens de la population de l'est de la mer de Beaufort réalisés en 2019. Secr. can. des avis sci. du MPO. Doc. de rech. 2025/006. iv + 44 p.*

TABLE OF CONTENTS

ABSTRACT

Beluga whales (*Delphinapterus leucas*) of the Eastern Beaufort Sea (EBS) population represent the second largest beluga population in Canada. The last abundance assessment for this population was conducted in 1992 through an aerial survey, which included coverage of the offshore Beaufort Sea, west Amundsen Gulf, and the inshore bays of the Mackenzie estuary. In July 2019, Fisheries and Oceans Canada conducted an aerial survey of the Eastern Beaufort Sea beluga population using a visual survey of offshore waters of the Beaufort Sea, Amundsen Gulf, and Prince of Wales Strait, and a photographic survey for inshore of the Mackenzie estuary. The objectives of this study are to 1) update the abundance estimate for this beluga population with the July 2019 survey data and 2) calculate the Potential Biological Removal. The total abundance estimate for the EBS beluga population in Canadian waters in July 2019 was of 38,451 belugas (CV = 0.327, 95% CI = 20,735–71,304). The associated Potential Biological Removal was estimated to be 588 belugas.

INTRODUCTION

The Eastern Beaufort Sea (EBS) beluga whale (*Delphinapterus leucas*) population migrates from the Bering Sea to the Beaufort Sea during spring, following the retreat of sea ice (Fraker 1979, Asselin et al. 2011, Hornby et al. 2016). Belugas typically enter the shallow bays of the Mackenzie River estuary in July, where previous aerial surveys have estimated aggregations of ~ 2,000 whales in these areas (Norton and Harwood 1986, Harwood et al. 1996). Based on telemetry studies, the summer range of EBS beluga includes areas of the Beaufort Sea continental shelf, Amundsen Gulf, and Viscount Melville Sound (Richard et al. 2001, Storrie et al. 2022). Throughout the summer, Inuvialuit communities harvest beluga whales, at coastal whaling camps along the Mackenzie estuary by the communities of Inuvik, Aklavik, and Tuktoyaktuk, and also opportunistically offshore by harvesters from Paulatuk, Ulukhaktok, and Sachs Harbour (Day 2002, Harwood et al. 2015, Harwood et al. 2020).

The last Canadian population abundance assessment for the EBS beluga population was conducted in 1992 by Fisheries and Oceans Canada (DFO) (raw sighting data in Harwood and Norton 1996). The survey covered the Beaufort Sea shelf and the western Amundsen Gulf, as well as Shallow Bay, East and West Mackenzie Bays, and Kugmallit Bay (Harwood et al. 1996). Analysis of the survey data produced an abundance estimate of 19,629 (95% CI = 15,134–24,125) belugas observed at the surface (Harwood et al. 1996). That estimate was corrected by Duval et al. (1993) and Angliss and Outlaw (2005) using a factor of two, to account for whales that were under the surface of the water during the survey and thus unavailable to be counted, resulting in an estimate of 39,258 belugas. The 1992 population estimate was considered to be conservative as the survey did not cover the entire known summer range of the EBS beluga population (Muto et al. 2018). The population has previously been assessed as “not at risk” by the Committee on the Status of Endangered Wildlife in Canada (COSEWIC 2004), and stable or increasing by DFO (2000). The objectives of this study are to:

1. Estimate and update the EBS beluga abundance in Canadian waters using aerial survey data collected by DFO (July 2019).
2. Calculate Potential Biological Removal (PBR) using the best available information.

METHOD

STUDY AREA AND SURVEY DESIGN

As part of a collaborative approach with Inuvialuit co-management partners, a community tour of all six communities of the Inuvialuit Settlement Region was held in November 2018 to share proposed areas of interest and logistical plans for the 2019 aerial survey. In each community the design of the strata and transect lines, as well as the timing of the survey, were presented and discussed. Survey design was also discussed with the Fisheries Joint Management Committee and the Inuvialuit Game Council. The survey coverage (Longitude = 141°W to 115°W; Latitude = 69°N to 73°N) was designed to cover similar strata flown in the 1992 aerial survey (Mackenzie Bays, Beaufort shelf and west Amundsen Gulf) (Harwood et al. 1996) and sought to extend the survey area to include a greater portion of the summer range (adding east of Amundsen Gulf, Prince of Wales Strait, west Banks Island) based on past and 2018 telemetry studies (Richard et al. 2001, Storrie et al. 2022), and following the consultations with Inuvialuit representatives (MacPhee et al. 2025a,b; Figure 1). To optimize survey design and cover more area, transect lines were designed as zig-zag lines, with 20 km spacing in the Beaufort offshore stratum, 40 km in the Amundsen Gulf and in Prince of Wales Strait. The lines for the eastern part of the Beaufort offshore were also redesigned during the survey to systematic parallel lines, consistent with the 1992 survey, with 30 km spacing, to allow more time for the observers to rest between transects. Only a photographic survey was conducted in the inshore stratum of east Mackenzie estuary due to the expected higher beluga density in the area. Lines inshore were also systematic parallel lines with 5 km spacing (Longitude = 137.72°W to 133.05°W; Latitude = 68.90°N to 69.61°N) (Figure 2).

VISUAL SURVEY – JULY

The survey was planned to occur from 17 July to 2 August 2019. Two de Havilland Twin Otter aircraft were used to fly the survey. Four visual observers were seated at bubble windows on each side of the aircraft, two at the front and two at the rear. Observers always stayed in the same position. A Bad Elf GPS Pro+ unit logged position, altitude, speed, and heading of the aircraft every second. Transect lines were flown at a target altitude of 1,000 ft (305 m) and target speed of 100–110 knots (185–204 km/h). Aircrafts were flown on days with optimal conditions: no rain, no risk of icing, ceiling of 1,000 ft or higher, minimal fog over water and forecasted or actual Beaufort Scale of Wind Force of 3 or less. The visual survey transects were truncated at the northern limit when sea ice concentration was 80–100% or fog obliterated the search area.

The survey used double-platform line-transect survey protocols, with a pair of independent observers on each side of the plane (Buckland et al. 2001). To ensure independence between the front and rear observer teams while on the transect, observers were acoustically isolated with noise cancelling Bose A20 aviation headsets and visually isolated by a black curtain hung in the middle of the plane. To record declination angle, observers used Geometers V2 from Pi Technology (Pi Technology, Seltjarnarnes, Iceland). This device provides more accurate measures than clinometers (used in previous survey) and simultaneously records GPS locations, time, and perpendicular declination angle of a sighting (individual beluga or middle of a beluga group). Each observer had a geometer connected via USB to a Microsoft Surface Pro tablet, with the geometer Pi Attitude software (Hansen et al. 2020), and was also connected to a GPS Bad Elf+ to geo-reference each sighting. Observers dictated and recorded the information for their sightings with their headset, connected via Bluetooth to the tablet and Pi Attitude software as well. Observers were instructed to concentrate their search effort near the transect line under the plane. For visible belugas at or near the surface (see AVAILABILITY BIAS CORRECTION section below), observers dictated the estimated group size (whales within 2 body lengths of each other, Doniol-Valcroze et al. 2015), and when possible, presence of calves, swimming direction (clock system), and behaviour (surfacing, diving, feeding, etc.). Primary observers (at the front) also recorded environmental conditions such as Beaufort Scale of Wind Force (Beaufort scale), ice concentration (in tenths), glare intensity (none, light, medium, high), direction of glare (clock system), and fog coverage (% of field of view).

Visual survey observers participated in a one-day training on July 17 and practiced survey protocols/technical equipment during a practice flight. They also participated in a pool-based egress training course.

VISUAL SURVEY – AUGUST

The National Oceanic and Atmospheric Administration (NOAA) of the United States also conducted an aerial survey in the Beaufort area during the summer of 2019 with the main objective to estimate the size of the Bering-Chukchi-Beaufort Seas bowhead whale (*Balaena mysticetus*) population (Figure 3). However, in addition to counting bowhead whales during the survey, observers also counted belugas. The portion of the visual survey within Canadian borders was conducted from August 8 to August 27. Comprehensive field methods and a summary of results for the NOAA survey can be found in (Clarke et al. 2020). In brief, survey protocols were similar to the July DFO survey with the following deviations. NOAA surveys were flown in two Turbo Commander aircraft and a De Havilland Twin Otter. All aircraft were equipped with bubble windows for the front observers. Additionally, one Turbo Commander aircraft had a downward-pointing digital single lens reflex camera with a 20- or 21-mm lens mounted to the belly that collected true color (red, green, and blue [RGB]) imagery (Clarke et al. 2019, Clarke et al. 2020). The imagery served as an independent observer for a mark-recapture analysis of the NOAA aerial observer data. Transects were spaced 18 km apart with target airspeed at 213 km/h (115 knots). Target altitude was 396 m (1,300 ft), but the survey could be flown as low as 305 m (1,000 ft) if needed. The NOAA survey defined a sighting to be all whales within 5 body lengths of each other.

PHOTOGRAPHIC SURVEY – JULY

The inshore strata (Mackenzie Bay, Kugmallit Bay and Shallow Bay) were covered by the same two Twin Otter aircrafts or by a Remotely Piloted Aircraft System (RPAS), the Griffon SeaHunter aircraft (tail sign N372UA) operated by the University of Fairbanks Alaska (for more details see Jurjen van der Sluijs et al. 2023). Both types of aircraft were equipped with a Nikon D850 camera with a 25-mm lens mounted in a camera hatch, facing straight down, with the longest side perpendicular to the transect lines. The RPAS and Twin Otters were flown at a target altitude of 610 m (2,000 ft) and target speed of 185–204 km/h (100–110 knots). For the Twin Otters, the cameras were operated and settings (shutter speed, aperture, and capture interval) were adjusted remotely through the Nikon Camera Control Pro 2 software on a laptop computer inside the plane. The camera in the RPAS was set to automated settings. Each photograph was geotagged via Bluetooth GPS receiver uplink (Bald Elf GSP Pro+ linked to Unleashed D200+ Bluetooth Module).

Photographs for the inshore transects covered approximately 510,125 m^2/photograph ($875\ m \times 583\ m$) and were captured at a continuous interval of 7 sec, to allow ~20% overlap.

ANALYSIS

VISUAL SURVEY – JULY

For each observer, audio recordings of sightings were matched with the geometer data based on timestamp, and the altitude and declination angles were used to calculate the perpendicular distance of groups of belugas to the transect line. In both planes, the secondary observers on the right side had technical difficulties throughout the survey, resulting in a high proportion of missing data. From July 31 until the end of the first survey (August 2), two of the Inuvialuit observers stayed in Ulukhaktok, while the rest of the team transited back to Inuvik, leaving plane 2 with only the primary observers. As a result, we were limited to perform single platform distance analyses on the primary observer data only, and to use the double-platform data to estimate the probability of detection at the transect line (p(0), one source of perception bias) of the primary observers. Lastly, we fitted density surface models (DSM) to the sighting data. However, the DSMs fitted poorly to the observation data and the deviance explained by the model was low (<65%). Therefore, we decided against the use of the density surface model approach (but see Appendix A for more information on the DSM analysis and results).

Analyses were conducted in R v.4.1.2 (R Core Team 2022) with the packages “mrds” (Laake et al. 2022) for the mark-recapture distance sampling (MRDS) analysis, “Distance” (Miller 2022) for the multiple covariates distance sampling (MCDS) analysis, and “dsm” for the density surface modelling (dsm) (Miller et al. 2022).

Detection function

A detection function was fitted on the perpendicular distance data from the primary observers with a MCDS analysis. Data were right truncated at 900 m because counts approached zero at that perpendicular distance (Figure 4). No left truncation was required because the bubble windows' size allowed observers to detect animals directly on the trackline. Half-normal and hazard-rate key functions were tested, including cosine, polynomial, or no adjustments. Covariates were tested as well, including the observer (obs), cluster size (size), Beaufort Scale (sea state), ice concentration (ice), glare intensity (glare) and plane. The model was selected based on the lowest Akaike information criterion (AIC) and simplest model (model with fewest covariates if ΔAIC < 2). Goodness of fit was tested with a Cramer-von Mises test. The effective strip half-width, or the distance from the line at which as many objects are seen beyond that distance as are missed within the distance, was also calculated for comparison with other surveys.

The beluga encounter rate and its associated variance were estimated using a post-stratification scheme (variance estimator 'R2'; Fewster et al. 2009). Beluga density estimates were calculated per stratum based on equation 3.67 in Buckland et al. (2001) and the total estimate per stratum was calculated by multiplying beluga density by stratum area.

Mark-Recapture Distance Sampling

One key assumption of distance sampling analysis is that the probability of detection of whales at the track line (p(0)) is 1. However, observers may miss whales that were visible at the surface (perception bias). Although the detection function also partly corrects for perception bias by accounting for the effects of distance and possibly other covariates on detection of available animals, calculating the actual value of p(0) can be used to scale the intercept of the detection function. Therefore a MRDS analysis was performed to estimate the value of p(0), including only observers from one side of the plane and only the days that the planes flew with a double platform (Table 1).

For the transects conducted in double platform survey mode, duplicated sightings were identified based on the time between the two observations (<10 sec, except for five observations of 12, 13 or 15 sec) (e.g., Asselin et al. 2012, Watt et al. 2020). Other measurements like group size, angle (<8 degrees, except for 11 observations), and GPS coordinates were also used to confirm in case of ambiguity. Context and clear information allowed us to confidently identify the few duplicates beyond the predefined thresholds. For duplicated observations, the average distance abeam of the two observers were used to fit the detection function.

For the MRDS analysis, the independent observer configuration with point independence model (Burt et al. 2014, Buckland et al. 2015) was used with a 900 m right-truncation distance. Half-normal, hazard-rate, and gamma key functions were tested, as well as the following covariates: cluster size (size), Beaufort Scale (sea state), ice concentration (ice), glare intensity (glare) and plane. The best model was selected based on the lowest AIC. A Cramer-von Mises test was used to check the goodness of fit of the selected model. Lastly, we calculated the probability of detection on the trackline, p(0), of the primary observers to use as correction factor in the single platform distance sampling analysis (above) where the surface abundance estimate calculated from the primary observers' data was multiplied by 1/p(0).

VISUAL SURVEY – AUGUST

NOAA is presently working with their co-management partners, the Alaska Beluga Whale Committee, to refine the correction factors necessary to derive an estimate of population abundance from their 2019 aerial line-transect survey data. Therefore, an estimate of EBS beluga population abundance from the 2019 NOAA survey is not available at this time. However, we compared beluga encounter rates (number of belugas per km surveyed), an index of relative abundance, within strata derived from the NOAA 2019 survey data and the DFO data.

PHOTOGRAPHIC SURVEY – JULY

The aircraft and RPAS successfully surveyed Shallow Bay, Kugmallit Bay, and Mackenzie Bay (Figure 5B, Table 1). Photographs were examined for beluga by a photo reader experienced in analysing aerial photos from two previous DFO monodontid surveys (Charry et al. 2018, Watt et al. 2021). The photo reader was first given an initial set of 30 photographs (containing 370 belugas) that were previously analysed as part of another beluga survey. An agreement of 80% needed to be reached before the observer could start reading the new photos; this level of proficiency was achieved after reading an additional set of 10 photographs (containing 88 belugas).

Photographs were georeferenced and examined in ArcMap 10.1 (Esri). Issues with low visibility in images due to darkness were resolved using Adobe PhotoShop (Adobe Systems) by adjusting photograph brightness, contrast, levels, curves, exposure, vibrance, saturation, and hue. Water clarity was subjectively evaluated in each photo and classified as either ‘murky’ (water in which belugas could only be observed at the surface) or ‘clear’ (water in which belugas could be observed under the surface of the water). On some photos, a proportion of the photo was masked by sun glare which made it impossible for the reader to evaluate the presence of belugas. For those photos, the photo reader created a shapefile to cover the glare and did not search for belugas within the glare area. The area covered by the glare was then calculated and subtracted from the photo area. The overlapping section between subsequent photos was cropped from the first photo and belugas were not counted in the cropped section. Lastly, land area was cropped from the photos by overlapping a shapefile of land with the photos. The remaining area covered by water (with no glare) in each photo was then calculated.

A strip transect analysis of the individual beluga (not group) detections from the photos for the inshore strata was performed. The density of belugas was calculated by dividing beluga counts by the total area of glare-free water. Density was then multiplied by the stratum area to obtain near-surface abundance estimates $\widehat{N}_{sur}$ for each stratum. The variance of the encounter rate was calculated following equation variance estimator ‘R2’ in Fewster et al. (2009). For one stratum that was repeated, we averaged the abundance estimates weighted by effort and the variance of the average was calculated with equation 8.8 in Buckland et al. (2001).

AVAILABILITY BIAS CORRECTION

Aerial survey observers and photo analysts can only count belugas that are visible near or at the surface and within the observers’ field of view. Based on a previous experiment with modeled live-sized belugas, it was estimated that adult belugas were visible from our plane at depths up to 5 m in clear water (Richard et al. 1994). It was assumed that belugas in murky waters, such as those in estuaries, can only be seen at depth up to 2 m (Richard 2013). Therefore, surface estimates of beluga abundance had to account for the availability bias (i.e., the proportion of animals that occur at depths not visible to observers; Marsh and Sinclair 1989).

We used correction factors (C_a) based on 13 belugas tagged in 2018–2019 in the Eastern Beaufort Sea (Marcoux et al. 2025). Two different correction factors were used depending on the location, water turbidity, and on the time that observers had to detect belugas (instantaneous in photographic survey and non-instantaneous in visual survey). For belugas found in the inshore areas that are also murky and were surveyed by photographic methods, we used an instantaneous correction factor based on data from belugas that visited the inshore strata of the survey (Mackenzie Bay, Kugmallit Bay and Shallow Bay). The inshore correction factor was based on the time that belugas spent at the surface of the water (within 1 m; C_{aI} =1.56, S.D.= 0.592). For areas where the water was clearer (offshore) and were covered by visual observations, we used a correction factor based on the proportion of time belugas in the offshore survey strata spent in the top 5 m of water. This offshore correction factor was calculated using the Laake equation (Laake et al. 1997) to account for time that visual observers have to detect animals based on the speed of the plane and the viewing angle estimated at 14 sec, and resulted in C_{aLaake} = 1.94 (S.D. = 0.521; see Marcoux et al. 2025 for more detail on calculations).

POPULATION ABUNDANCE ESTIMATION

Near-surface abundance estimates of beluga in each stratum were adjusted to account for diving belugas which were not available to be observed (see AVAILABILITY BIAS CALCULATION section).

$$\widehat{N} = \widehat{N}_{sur} \times C_a$$

where C_a is the availability bias correction factor (for the inshore or offshore strata) and $\widehat{N}$ is the adjusted abundance estimate.

The final abundance estimate had an associated variance calculated using the delta method (equation 3.4, Buckland et al. 2001) and included variance from the encounter rate, group size, effective strip half-width, availability bias, and probability of detection at distance 0 for the visual survey, and the variance from the encounter rate and availability bias for the photographic survey.

The coefficient of variation (CV) was calculated by dividing the square root of the variance (standard error, SE) by the estimated abundance.

Population abundance was estimated by summing the abundance estimates (and their associated variances) adjusted for availability and perception biases of the individual stratum of the DFO July survey. 95% confidence intervals (CI) were calculated assuming a log-normal distribution (equation 3.71, Buckland et al. 2001).

POTENTIAL BIOLOGICAL REMOVAL

The PBR method (Wade 1998) was used to calculate sustainable level of removal for the population:

$$PBR = 0.5 \times R_{max} \times N_{min} \times F_r$$

Where $Rmax$ is the maximum rate of increase for the stock (which is unknown, therefore the default for cetaceans of 0.04 was used; Wade 1998), $Nmin$ is the 20th percentile of the log-normal distribution of N and Fr is the recovery factor which is set between 0.1 and 1 (Wade 1998). Here, Fr = 1 was used because the population is abundant and stable, and its assessed by the COSEWIC (2004) as *Not at Risk* (Hammill et al. 2017).

RESULTS

VISUAL SURVEY – OFFSHORE

A practice flight was done on 17 July to test equipment and protocols. The survey was conducted over 7 days from 21 July to 2 August 2019. On 21–23 July, we only operated one of the two aircraft due to technical issues and low cloud coverage. Weather conditions lead to interruptions and gaps in the planned survey direction and progression. The survey coverage was split into four strata: Beaufort offshore West (BOW) and East (BOE), Amundsen Gulf East (AGE) and Prince of Wales Strait South (WS) (Figure 1). Transects further north in WS stratum were also flown but were removed due to high ice concentration (close to 100%) which meant that no belugas could be present in the area.

In total, 31 individual transect lines were flown in the offshore Beaufort Sea, with varying environmental conditions: Beaufort Scale with sea states from 1 to 3, ice concentration from 0–70%, and glare intensity of none to medium (Table 1). A total of 278 belugas (195 groups) were observed by the four primary observers over these four strata, for a total effort of 3,470 km (5.6% area covered, Table 2, Figure 5). The time difference between when an observer detected a group of belugas and when the group was abeam of the aircraft (also called time-in-view) ranged from 0 to 13 sec (Mean = 2.88 sec, SD = 2.66, SE = 0.19, Figure 6).

Multiple Covariates Distance Sampling

The best MCDS model when considering the primary observer data (single platform) had a half-normal key function with glare as a covariate and resulted in an effective strip half-width of 406.8 m (Table 3, Figure 7).

Mark-Recapture Distance Sampling

The best distance sampling model was described by a half-normal detection function with no covariates and the mark-recapture model included the covariates distance and plane (Table 4). The detection probability for the primary observer on the left side of both planes, p(0), was 0.565 (SE = 0.095, CV = 0.168; Table 5).

Correction for availability and perception bias

We corrected surface estimates for perception bias by multiplying the estimates by the inverse of the detectability probability from the MRDS (1/p(0) = 1.77). The correction factor for availability bias (C_{aLaake} = 1.94, SD = 0.521) was set as a multiplier to the surface abundance estimate. The total corrected estimate for the offshore areas was 35,738 belugas (95% CI = 17,891–71,387, Table 6).

August aerial survey by the National Oceanic and Atmospheric Administration

Strata for the NOAA survey in the EBS were generated to match as closely as possible the strata of the July survey. The core areas surveyed were: Beaufort offshore West (BOW) and East (BOE), Amundsen Gulf West (AGW) and East (AGE), and West of Banks Island (WBI) (Figure 3). A total of 47 individual transect lines were flown. The August survey covered 152,529 km^2 and 799 belugas were sighted (546 groups) (Table 7, Figure 8). The highest beluga encounter rates were found in the AGW stratum and the lowest were in the WBI stratum (Table 7).

PHOTOGRAPHIC SURVEY – INSHORE

The two Twin Otter aircrafts flew a total of 39 transect lines in the inshore area on 23 July and 2 August (Figure 5). The RPAS flew across the Shallow Bay stratum on 28 July (Table 1). Since the Shallow Bay stratum was repeated, we took the average of two abundance estimates weighted by effort (total area covered by photos) similar to other aerial survey estimate calculations (Marcoux et al. 2016, Gosselin et al. 2017). The total surface estimate for the inshore areas was 1,740 belugas. This estimate was corrected for the availability bias correction factor for the inshore area based on the time belugas spent in the top 1 metre (C_{aI} =1.56, SD = 0.592). The corrected estimate was 2,714 (CV = 0.30, 95% CI = 1,518–4,850, Table 8).

POPULATION ABUNDANCE ESTIMATION AND ASSOCIATED POTENTIAL BIOLOGICAL REMOVAL (PBR)

The total abundance estimate for the EBS beluga population is of 38,541 (CV = 0.327, 95% CI = 20,735–71,304, Table 9). The associated PBR was estimated at 588 belugas based on a N_{min} of 29,400 belugas and a recovery factor of 1.

DISCUSSION

BELUGA DISTRIBUTION

The 2019 DFO survey was conducted over a 13-day period, with seven days of suitable weather conditions for surveying. It is possible that belugas made systematic movements between and beyond strata during that period (Richard et al. 2001) and that our assumption of random movement of belugas was violated. However, the orientation of beluga groups in the photos that were taken simultaneously during the survey did not indicate a general bearing or movement toward one direction (Mayette et al. 2022). Within the surveyed area, belugas were found in higher density in the Beaufort offshore stratum, especially West and around the Tuktoyaktuk Peninsula in July (Table 9, Figure 5). In comparison, belugas were in higher density in Amundsen Gulf West during the August survey (Figure 8, Clarke et al. 2020), typical of their August distribution. EBS belugas have been observed to move east in early August and start the fall migration back west in September (Richard et al. 2001, Storrie et al. 2022). However, the Amundsen Gulf West stratum was not surveyed during the 2019 July survey, which makes it impossible to compare or show an eastward movement between the two months.

The survey was designed to observe belugas in high aggregations close to the shore and in the Mackenzie estuary in the month of July. However, we did not encounter the expected large aggregations in the inshore areas of the survey. In addition, group size (range from 1–8) was observed to be smaller than in the previous survey in 1992 (range from 1–22; Harwood et al. 1996, Mayette et al. 2022). There was also a shift in distribution towards the interior of Mackenzie estuary compared to in the 1990s (Noel et al. 2022). Storms and high winds are known to drive belugas to swim closer to the coast, and in estuaries, they sometimes swim upriver (Scharffenberg et al. 2020a). Specifically, strong winds were recorded at Shingle Point (in the Shallow Bay stratum; up to 68 km/h) and Tuktoyaktuk (in the Kugmallit Bay stratum; up to 57 km/h) during the night of 20 to 21 July 2019, two days before Kugmallit Bay and Shallow Bay were surveyed (Mayette et al. 2022). Detection rate recorded by hydrophones showed a decrease in beluga calls in two recording stations located in Kugmallit Bay, on July 23 compared to the average of the three previous weeks (July 1–21) (West Hendrickson: from 17.9 pulsed detections per minute (DPM) to 1.6 DPM, and East Whitefish: from 9.5 DPM to 3.3 DPM (Scharffenberg et al. 2025). Given that belugas leave the inshore area to take refuge offshore during storm events and during hunting, and can take up to five days to return (Scharffenberg et al. 2020b), this weather event would have influenced the distribution, presence and abundance of beluga in the inshore estuary strata at the time of the survey.

For most beluga populations, a large proportion of the population tends to summer in high density areas in estuaries or near the coast (e.g., Lowry et al. 2017, Matthews et al. 2017, Watt et al. 2021). Consequently, aerial surveys for these populations are designed to cover the high density areas with high or full coverage during this time. For example, 99.9% of the Western Hudson Bay belugas were found in the river estuaries and coastal areas of the 2015 aerial survey (Matthew et al. 2017). During the 2014 and 2017 surveys, 75% of the Cumberland Sound belugas were found in fiords including Clearwater Fiord, and aerial surveys were designed to fully cover that area (Marcoux et al. 2016, Watt et al. 2021). The summer distribution of the EBS beluga population is atypical from other small Arctic cetaceans since a large portion of the population is typically found in the offshore areas in low density, at the same time that a portion of the population is aggregated within the estuary. In addition, the offshore may be becoming more attractive to EBS belugas due to increased prey availability (Hornby et al. 2017). During the 1992 survey, over 85% of belugas were found offshore, compared to inshore (Harwood et al. 1996; Figure 9). In the 2019 survey, 91% of belugas were found in the offshore. Therefore, it is challenging to cover the entire summer distribution of the EBS population, compared to other beluga populations, resulting in less precise and accurate survey estimates than if the population was concentrated in a smaller area.

ABUNDANCE ESTIMATES COMPARISON

When comparing the results of the single platform analyses from the 1992 and 2019 (this study) surveys, with estimates corrected for perception and availability biases (Table 9), we notice similar abundance estimates that are within each others 95% CI. However, the area covered by the 2019 survey strata was larger than in 1992 (+50.5% covered area, Table 10, Figure 10). As a consequence, the density of belugas was lower in the 2019 survey. The encounter rate of the DFO July 2019 survey was also lower than the NOAA August 2019 survey.

LIMITATIONS

Limited flying time due to weather challenges led to incomplete and interrupted timing of survey coverage (Figure B1). Other sources of information (i.e., telemetry data, local knowledge) have indicated that belugas were present in areas that were not surveyed. Thus, it was not possible to estimate the proportions of belugas in the areas not covered by the 2019 survey, especially given that most of the missing areas had not previously been surveyed. Since only a portion of the EBS beluga population was surveyed, the abundance estimate provided from this survey is considered an underestimate.

The availability bias adjustment factor used for this survey was based on the diving behaviour of eight male belugas equipped with satellite transmitters in 2018 and 2019 from a single capture location. For this study, we assumed that the behaviour of the tagged belugas was representative of the belugas observed during the 2019 aerial surveys. However, beluga diving behaviour is known to vary by sex, activity state and habitat, and females with calves are likely to spend more time at the surface than males. As a result, the availability bias adjustment used likely resulted in a positive bias in the abundance estimate.

In addition, the availability adjustment factor used in this study was based on individual beluga diving behaviour and does not take into account that belugas were encountered in groups during the visual survey. There is uncertainty on synchronicity of the diving behaviour of belugas within a group. However, it is likely that belugas do not dive in perfect synchrony and that the availability adjustment factor used resulted in a positive bias of the abundance estimate.

The estimate of total abundance was based on the sum of the abundances of the strata surveyed over a period of thirteen days and in a discontinuous order. We assumed that the movement of belugas among strata was random, which would produce unbiased abundance estimates. However, we did not assess whether directed movements among strata occurred during the survey period. In addition, the inshore areas were surveyed at the start of August when belugas are known to leave the Mackenzie estuary and disperse offshore. It is not clear how these factors could have biased the survey estimate.

Environmental changes in the Canadian Beaufort Sea likely resulted in change in beluga distribution and grouping pattern in 2019 compared to previous survey years. In particular, 2019 was an anomalous warm year based on spring sea ice break-up timing, sea surface temperatures and local hunter observations. The year 2019 was also marked by an unusually high number of mortalities of marine animals in the Canadian Beaufort Sea (DFO unpublished data). Lastly, storms and high winds in the inshore areas resulted in high wave activity and possible displacement of beluga whales from the Mackenzie estuary during the time of the survey.

During the July 2019 survey, the observers tested new equipment to increase precision in the declination angle reading. Overall, the new geometers were a successful new addition in the methodology, and we are satisfied with the precision of the angle reading. However, there were some technical difficulties at the beginning of the survey, which caused missing recordings along transects, complications in the duplicate identification, and removal of observations from the final analysis. The long length of many offshore transect lines (> one hour to complete) also made it challenging for observers, who can feel tired after a long period of focus and more technical problems can occur (i.e., losing GPS connection, geometers going to sleep, recording cutting, etc.).

ACKNOWLEDGEMENTS

We thank the aerial survey team, including the local observers from Inuvik (A. Gordon and B. Joe) and Ulukhaktok (B. Okheena and R. Inuktalik), R. McLeod and K. Barr from the Aurora Research Institute, the DFO crew (C. Hornby, D. Yurkowski, C. Hoover, D. Neumann, and C. Debets), and pilots and crew from Kenn-Borek (M. Whitley, K. Turner, C. Callaway and A. de Boer). We thank A. Brower from NOAA for their help and collaboration with the August survey. We also thank the Inuvialuit Game Council, the Fisheries Joint Management Committee, and the Hunters and Trappers Committees for their support as well as Whale Seeker for the photo detection analysis.

REFERENCES CITED

Angliss, R.P., and Outlaw, R.B. 2005. Beluga whale (*Delphinapterus leucas*): Beaufort Sea stock. Alaska Marine Mammal Stock Assessment. NOAA-TM-AFSC-161. 6 p.

Asselin, N.C., Barber, D.G., Stirling, I., Ferguson, S.H., and Richard, P.R. 2011. Beluga (*Delphinapterus leucas*) habitat selection in the eastern Beaufort Sea in spring, 1975–1979. Polar Biol. 34: 1973–1988.

Asselin, N.C., Ferguson, S.H., Richard, P.R. and Barber, D.G. 2012. Results of narwhal (*Monodon monoceros*) aerial surveys in northern Hudson Bay, August 2011. DFO Can. Sci. Advis. Sec. Res. Doc. 2012/037. iii + 23 p.

Buckland, S.T., Anderson, D.R., Burnham, K.P., Laake, J.L., Borchers, D.L., and Thomas, L. 2001. Introduction to distance sampling: estimating abundance of biological populations. Oxford University Press, Oxford, U.K. 448 p.

Buckland, S.T., Rexstad, E.A., Marques, T.A., and Oedekoven, C.S. 2015. Distance sampling: methods and applications. *Edited by* A.P. Robinson, S.T. Buckland, P. Reich and M. McCarthy. Springer International Publishing, Cham. xv + 277 p.

Burt, M.L., Borchers, D.L., Jenkins, K.J., and Marques, T.A. 2014. Using mark-recapture distance sampling methods on line transect surveys. Methods Ecol. Evol. 5(11): 1180–1191.

Charry, B., Marcoux, M., and Humphries, M.M. 2018. Aerial photographic identification of narwhal (*Monodon monoceros*) newborns and their spatial proximity to the nearest adult female. Arct. Sci. 4(4): 513–524.

Clarke, J.T., Brower, A.A., Ferguson, M.C., and Willoughby, A.L. 2019. Distribution and relative abundance of marine mammals in the Eastern Chukchi and Western Beaufort Seas, 2018, annual report. National Marine Fisheries Service, Alaska Fisheries Science Center (U.S.), Marine Mammal Laboratory (U.S.), and Bureau of Ocean Energy Management, Seattle, WA.

Clarke, J.T., Brower, A.A., Ferguson, M.C., Willoughby, A.L. and Rotrock, A.D. 2020. Distribution and relative abundance of marine mammals in the Eastern Chukchi Sea, Eastern and Western Beaufort Sea, and Amundsen Gulf, 2019, annual report. National Marine Fisheries Service, Alaska Fisheries Science Center (U.S.), Marine Mammal Laboratory (U.S.), and Bureau of Ocean Energy Management, Seattle, WA.

COSEWIC. 2004. COSEWIC assessment and update status report on the Beluga whale Delphinapterus leucas in Canada. Committee on the Status of Endangered Wildlife in Canada. Ottawa. ix + 70 pp.

Day, B. 2002. Renewable resources of the Beaufort Sea for our children: perspectives from an Inuvialuit elder. Arctic. 55(Supplement 1): 1–3.

DFO. 2000. Eastern Beaufort Sea Beluga. DFO Science Stock Status Report E5-38 (2000).

Doniol-Valcroze, T., Gosselin, J.F., Pike, D., Lawson, J., Asselin, N., Hedges, K., and Ferguson, S. 2015. Abundance estimates of narwhal stocks in the Canadian High Arctic in 2013. DFO Can. Sci. Advis. Sec. Res. Doc. 2015/060. v + 36 p. (Erratum April 2022)

Duval, W.S. 1993. Proceedings of a workshop on Beaufort Sea beluga: February 3-6, 1992. Vancouver, B.C. Environmental Studies Research Funds Report No. 123. Calgary. 33 p. plus appendix.

Fewster, R.M., Buckland, S.T., Burnham, K.P., Borchers, D.L., Jupp, P.E., Laake, J.L., and Thomas, L. 2009. Estimating the encounter rate variance in distance sampling. Biometrics. 65(1): 225–236.

Fraker, M.A. 1979. Spring migration of bowhead (*Balaena mysticetus*) and white whales (*Delphinapterus leucas*) in the Beaufort Sea. Can. Fish. Mar. Serv. Tech. Rep. 859: vi + 36 p.

Gosselin, J.-F., Hammill, M.O., and Mosnier, A. 2017. Indices of abundance for beluga (*Delphinapterus leucas*) in James Bay and eastern Hudson Bay in summer 2015. DFO Can. Sci. Advis. Sec. Res. Doc. 2017/067. iv + 25 p.

Hammill, M.O., Stenson, G.B., and Doniol-Valcroze., T. 2017. A management framework for Nunavik beluga. DFO Can. Sci. Advis. Sec. Res. Doc. 2017/060. v + 34 p.

Hansen, R.G., Pike, D.G., Thorgilsson, B., Gunnlaugsson, T., and Lawson, J. 2020. The Geometer: a new device for recording angles in visual surveys. NAMMCO Sci. Publ 11: 9 p.

Harwood, L.A. and P. Norton. 1996. Aerial survey data from the southeast Beaufort Sea, Mackenzie River estuary and West Amundsen Gulf, July 1992. Can. Data Rep. Fish. Aquat. Sci. 965: iv + 25 p.

Harwood, L.A., Innes, S., Norton, P., and Kingsley, M.C.S. 1996. Distribution and abundance of beluga whales in the Mackenzie estuary, southeast Beaufort Sea and west Amundsen Gulf during late July 1992. Can. J. Fish. Aquat. Sci. 53: 2262–2273.

Harwood, L.A., Kingsley, M.C.S., and Pokiak, F. 2015. Monitoring beluga harvests in the Mackenzie Delta and near Paulatuk, NT, Canada: harvest efficiency and trend, size and sex of landed whales, and reproduction, 1970-2009. Can. Manuscr. Rep. Fish. Aquat. Sci. 3059: vi + 32 p.

Harwood, L.A., Zhu, X., Angasuk, L., Emaghok, L., Ferguson, S., Gruben, C., Gruben, P., Hall, P., Illasiak, J., Illasiak, J., Lennie, J, Lea, E.V., Loseto, L.L., Norton, P., Pokiak, C., Pokiak, F., Rogers, H., Snow, K., and Storr, W. 2020. Research, Monitoring and Hunter Knowledge in Support of the 2017 Assessment of the Eastern Beaufort Sea Beluga Stock. DFO Can. Sci. Advis. Sec. Res. Doc. 2020/075. v + 48 p.

Hornby, C.A., Iacozza, J., Hoover, C., Barber, D.G., and Loseto, L.L. 2016. Spring conditions and habitat use of beluga whales (*Delphinapterus leucas*) during arrival to the Mackenzie River Estuary. Polar Biol. 39: 2319–2334.

Hornby, C.A., Iacozza, J., Hoover, C., Barber, D.G., and Loseto, L.L. 2017. Beluga whale *Delphinapterus leucas* late summer habitat use and support for foraging areas in the Canadian Beaufort Sea. Mar. Ecol. Prog. Ser. 574: 243–257.

Laake, J.L., Calambokidis, J., Osmek, S.D., and Rugh, D.J. 1997. Probability of detecting harbor porpoise from aerial surveys: estimating g(0). J. Wildl. Manag. 61(1): 63–75.

Laake, J., Borchers, D., Thomas, L., Miller, D., Bishop, J., and McArthur, J. 2022. R package mrds: Mark-Recapture Distance Sampling (version 2.2.6).

Lowry, L., Zerbini, A., Frost, K., DeMaster, D., and Hobbs, R. 2017. Development of an abundance estimate for the eastern Bering Sea stock of beluga whales (*Delphinapterus leucas*). J. Cetacean Res. Manage. 16(1): 39–47.

MacPhee, S., Iacozza, J., Way-Nee, E., Inglangasuk, G., Pokiak, C., Lucas, J., and Loseto, L. 2025a. What We Heard: Summary of Community Meetings to Propose a New Beluga Tagging Program in the Inuvialuit Settlement Region. Can. Manuscr. Rep. Fish. Aquat. Sci. 3293: xi + 52 p.

MacPhee, S., Adams, B., George, J.C., Hansen, J., Inglangasuk, G., Kalinek, J., Marcoux, M., Murray, L., Loseto, L. 2025b. What We Heard: Community meetings for beluga and bowhead tagging and aerial survey programs planned for summer 2019 in the Inuvialuit Settlement Region. Can. Manuscr. Rep. Fish. Aquat. Sci. 3294: viii + 53 p.

Marcoux, M., Young, B.G., Asselin, N.C., Watt, C.A., Dunn, J.B., and Ferguson, S.H. 2016. Estimate of Cumberland Sound beluga (*Delphinapterus leucas*) population size from the 2014 visual and photographic aerial survey. DFO Can. Sci. Advis. Sec. Res. Doc. 2016/037. iv + 19 p. (Erratum: October 2016)

Marcoux, M., Storrie, L., MacPhee, S., and Loseto, L.L. 2025. Availability Bias Adjustment for Calculating Aerial Survey Abundance Estimates for Belugas (*Delphinapterus leucas*) in the Eastern Beaufort Sea. DFO Can. Sci. Advis. Sec. Res. Doc. 2025/002. iv + 23 p.

Marsh, H., and Sinclair, D.F. 1989. Correcting for visibility bias in strip transect aerial surveys of aquatic fauna. J. Wildl. Manag. 53(4): 1017–1024.

Matthews, C.J.D., Watt, C.A., Asselin, N.C., Dunn, J.B., Young, B.G., Montsion, L.M., Westdal, K.H., Hall, P.A., Orr, J.R., Ferguson, S.H., and Marcoux, M. 2017. Estimated abundance of the Western Hudson Bay beluga stock from the 2015 visual and photographic aerial survey. DFO Can. Sci. Advis. Sec. Res. Doc. 2017/061. v + 20 p.

Mayette, A., Loseto, L., Pearce, T., Hornby, C.A., and Marcoux, M. 2022. Group characteristics and spatial organization of the Eastern Beaufort Sea beluga whale (*Delphinapterus leucas*) population using aerial photographs. Can. J. Zool. 100(6): 363–375.

Miller, D.L. 2022. R package Distance: Distance Sampling Detection Function and Abundance Estimation (version 1.0.5).

Miller, D.L., Burt, M.L., Rexstad, E.A., and Thomas, L. 2013. Spatial models for distance sampling data: recent developments and future directions. Methods Ecol. Evol. 4(11): 1001–1010.

Miller, D.L., Rexstad, E., Burt, L., Bravington, M.V., Hedley, S., Ferguson, M., and Kelly, N. 2022. R package dsm: Density Surface Modelling of Distance Sampling Data (version 2.3.3).

Muto, M.M., Helker, V.T., Angliss, R.P., Allen, B.A., Boveng, P.L., Breiwick, J.M., Cameron, M.F., Clapham, P.J., Dahle, S.P., Dahlheim, M.E., Fadely, B.S., Ferguson, M.C., Fritz, L.W., Hobbs, R.C., Ivashchenko, Y.V., Kennedy, A.S., London, J.M., Mizroch, S.A., Ream, R.R., Richmond, E.L., Shelden, K.E.W., Towell, R.G., Wade, P.R., Waite, J.M., and Zerbini, A.N. 2018. Alaska marine mammal stock assessments, 2017. NOAA Tech. Memo. NMFS-AFSC-378. 382 p.

Noel, A., Devred, E., Iacozza, J., Marcoux, M., Hornby, C., and Loseto, L.L. 2022. Environmental drivers of beluga whales distribution in a changing climate: a case study of summering aggregations in the Mackenzie Estuary and Tarium Niryutait Marine Protected Area. Arct. Sci. 8(4): 1305–1319.

Norton, P. and L.A. Harwood. 1986. Distribution, abundance, and behaviour of white whales in the Mackenzie Estuary. Environmental Studies Revolving Funds, Report No. 036. Ottawa. 73 p.

Osborne, P.D. and Forest, A. 2016. Sediment dynamics from coast to slope – southern Canadian Beaufort Sea. J. Coast. Res. 75(10075): 537–541.

R Core Team. 2022. R: A language and environment for statistical computing. R Foundation for Statistical Computing. (version 4.1.2).

Richard, P.R. 2013. Size and trend of the Cumberland Sound beluga whale population, 1990 to 2009. DFO Can. Sci. Advis. Sec. Res. Doc. 2012/159. iii + 28 p.

Richard, P., Weaver, P., Dueck, L., and Baber, D. 1994. Distribution and numbers of Canadian High Arctic narwhals (*Monodon monoceros*) in August 1984. Medd. Grønl., Biosci. 39: 41–50.

Richard, P.R., Martin, A.R., and Orr, J.R. 2001. Summer and autumn movements of belugas of the Eastern Beaufort Sea stock. Arctic. 54(3): 223–236.

Scharffenberg, K.C., MacPhee, S.A., and Loseto, L.L. 2020a. Upriver sightings of beluga whales (*Delphinapterus leucas*) follow storm surges and high water in the Mackenzie Delta, Northwest Territories, Canada. Arct. Sci. 7(3): 679–689.

Scharffenberg, K.C., Whalen, D., MacPhee, S.A., Marcoux, M., Iacozza, J., Davoren, G., and Loseto, L.L. 2020b. Oceanographic, ecological, and socio-economic impacts of an unusual summer storm in the Mackenzie Estuary. Arct. Sci. 6(2): 62–76.

Scharffenberg, K, MacPhee, S., Mouy, X., Whalen, D., and Loseto, L. 2025. Automated Detection of Beluga Vocalizations in Kugmallit Bay in 2019 to Contextualize Results of Concurrent Aerial Surveys. Can. Tech. Rep. Fish. Aquat. Sci. 3557: vii + 9 p.

Storrie, L., Hussey, N.E., MacPhee, S.A., O'Corry-Crowe, G., Iacozza, J., Barber, D.G., Nunes, A., and Loseto, L.L. 2022. Year-round dive characteristics of male beluga whales from the Eastern Beaufort Sea population indicate seasonal shifts in foraging strategies. Front. Mar. Sci. 8: 715412.

van der Sluijs, J., Saiet, E., Bakelaar, C.N., Wentworth, A., Fraser, R.H., and Kokelj, S.V. 2023. Beyond visual-line-of-sight (BVLOS) drone operations for environmental and infrastructure monitoring: a case study in northwestern Canada. Drone Syst. Appl. 11: 1–15.

Wade, P.R. 1998. Calculating limits to the allowable human-caused mortality of cetaceans and pinnipeds. Mar. Mamm. Sci. 14(1): 1–37.

Watt, C.A., Hornby, C., and Hudson, J. 2020. Narwhal (*Monodon monoceros*) abundance estimate from the 2018 aerial survey of the Northern Hudson Bay population. DFO Can. Sci. Advis. Sec. Res. Doc. 2020/073. iv + 15 p.

Watt, C.A., Marcoux, M., Hammill, M.O., Montsion, L.M., Hornby, C., Charry, B., Dunn, J.B., Ghazal, M., Hobbs, R., Lee, D.S., Mosnier, A., and Matthews, C.J.D. 2021. Abundance and total allowable landed catch estimates from the 2017 aerial survey of the Cumberland Sound beluga (*Delphinapterus leucas*) population. DFO Can. Sci. Advis. Sec. Res. Doc 2021/050. iv + 33 p.

Weber, J.R. 1989. Physiography and Bathymetry of the Arctic Ocean seafloor. *In* The Arctic Seas: Climatology, Oceanography, Geology, and Biology. Edited by Y. Herman. Springer, Boston. pp. 797–828.

Wood, S.N. 2017. Generalized additive models: an introduction with R. 2e ed. CRC Press, Boca Raton, FL. 496 p.

Wood, S.N., Bravington, M.V., and Hedley, S.L. 2008. Soap film smoothing. J. Royal Statist. Soc. Ser. B. Statist. Methodol. 70(5): 931–955.

TABLES

Table 1. Summary of transect lines flown on each day of the survey, including the plane, the stratum (BOW: Beaufort offshore West, BOE: Beaufort offshore East, AGE: Amundsen Gulf East, WS: Prince of Wales Strait, SB: Shallow Bay, MB: Mackenzie Bay, KB: Kugmallit Bay), and transect line, the type of platform used for the analysis (single or double platform), and the environmental conditions (Beaufort sea state scale, ice concentration (%), and glare intensity (N: none, L: light, M: medium)).

Offshore								
Date	**Plane**	**Stratum**	**Transect**	**Left side**	**Right side**	**Beaufort scale**	**Ice conc. (%)**	**Glare**
21-Jul	2	BOW	5, 7	Double	Single	2, 3	0, 10–20	N, M
22-Jul	2	BOW	4, 6	Double	Single	1, 2	0, 10–20	N, L
23-Jul	2	BOE	1–4	Double	Single	1, 2, 3	0, 10–20	N, L
27-Jul	1	AGE	7–9	Double	Single	1, 2	0	L, M
28-Jul	2	WS	11–14	Double	Single	1, 2	10–20, 50–70	N, L
28-Jul	2	AGE	5, 6	Double	Single	2	0	L
31-Jul	1	BOE	11–15	Double	Single	1, 2	0	N
31-Jul	2	BOE	5–8	Single	Single	2, 3	0	N, L
02-Aug	1	BOE	9, 10	Double	Single	1	0	L, M
02-Aug	2	BOW	1–3	Single	Single	2	0	L, M

Inshore							
Date	**Plane**	**Stratum**	**Transect**	**Survey**	**Beaufort scale**	**Ice conc. (%)**	**Glare**
23-Jul	2	KB	1–10	Photographic	2, 3	0	N
28-Jul	RPAS	SB	1–13[a]	Photographic	1	0	L
28-Jul	RPAS	MB	1–10[a]	Photographic	2	0	L
02-Aug	1	MB	1–15	Photographic	2	0	L, M
02-Aug	2	SB	1–10	Photographic	2, 3	0	L, M
02-Aug	2	MB	16–19	Photographic	2	0	L, M

[a] The RPAS transects do not follow the same design as the aircraft transects (see Figure 2).

Table 2. *Survey effort of plane for each stratum (excluding observation outside of 900 m perpendicular distance from transect line): area of strata in km², distance flown on transect (effort in km), number of transect lines flown (k), area covered by transect (%), number of belugas observed (n) and number of groups (in parenthesis), mean group size, and encounter rate (ER, beluga per km) with standard error and coefficient of variation.*

Region	Area (km^2)	Effort (km)	k	Covered Area %	N	Mean size	ER	se(ER)	CV(ER)
AGE	35,250	663	5	3.39	33 (23)	1.43	0.0498	0.0098	0.198
BOE	55,341	1,913	15	6.22	170 (121)	1.40	0.0889	0.0266	0.299
BOW	14,713	649	7	7.94	66 (42)	1.57	0.102	0.0315	0.310
WS	6,202	245	4	7.12	9 (9)	1.00	0.0367	0.0080	0.217
Total	**111,506**	**3 470**	**31**	**5.60**	**278 (195)**	**1.43**	**0.0801**	**1.59e-5**	**0.198**

Table 3 Results of the top ten best model of multiple covariates distance sampling analysis. Key function used, covariates added to the formula, p-value of the Cramer-von Mises test (CvM p-value), the average detection probability ($\widehat{P}_a$), and its standard error ($se(\widehat{P}_a)$), the Akaike information criterion (AIC) and effective survey half-width (ESW in metres) are indicated. Selected model is shaded in grey.

	Key function	Formula	CvM *p*-value	$\widehat{P}_a$	$se(\widehat{P}_a)$	AIC	ΔAIC	ESW
1	Half-normal	~ glare	0.522	0.452	0.026	2,533.00	0	406.8
2	Half-normal	~ plane + glare	0.622	0.450	0.026	2,534.11	1.11	405
3	Half-normal	~ seastate + glare	0.608	0.447	0.025	2,534.39	1.39	402
4	Half-normal	~ size + glare	0.530	0.451	0.026	2,534.94	1.94	405.9
5	Hazard-rate (cos 2,3)	~ 1	0.928	0.376	0.036	2,535.44	2.44	338.4
6	Half-normal	~ plane + seastate + glare	0.684	0.446	0.025	2,535.87	2.87	401.4
7	Half-normal	~ obs + glare	0.581	0.447	0.026	2,535.97	2.97	402.3
8	Half-normal	~ obs + seastate + glare	0.568	0.441	0.026	2,536.05	3.05	396.9
9	Hazard-rate	~ seastate + glare	0.639	0.429	0.040	2,537.89	4.88	386.1
10	Hazard-rate	~ plane + glare	0.604	0.468	0.035	2,538.21	5.21	421.2

Table 4. Results of the top ten best models of mark-recapture (double platform) distance sampling analysis for the left side of both planes combined. DS model is the distance sampling model, which restricts the probability of detection at the survey line (p(0)) to be equal to 1, with associated Akaike information criterion (AIC_{DS}), the Average p_{DS} is the average detection probability. MR model are the mark-recapture models with associated Akaike information criterion (AIC_{MR}), the p(0) primary observer is the probability of a detected beluga at the transect line for the front left observer only, the combined AIC is the combined AIC of the MR and DS models, and ΔAIC is the difference in AIC score between the best model and the model being compared. Selected model is shaded in grey.

	Detection	**DS model**	**AIC_{DS}**	**Average p_{DS}**	**MR model**	**AIC_{MR}**	**p(0) primary observer**	**Combined AIC**	**ΔAIC**
1	Half-normal	~ 1	1,202.46	0.436 ± 0.037	~ distance + plane	192.35	0.565 ± 0.095	1,394.81	0
2	Half-normal	~ plane	1,203.62	0.434 ± 0.037	~ distance + plane	192.35	0.558 ± 0.097	1,395.97	1.16
3	Half-normal	~ obs	1,203.62	0.434 ± 0.037	~ distance + plane	192.35	0.558 ± 0.097	1,395.97	1.16
4	Half-normal	~ glare	1,203.95	0.430 ± 0.038	~ distance + plane	192.35	0.561 ± 0.096	1,396.30	1.49
5	Half-normal	~ size	1,203.98	0.435 ± 0.040	~ distance + plane	192.35	0.565 ± 0.095	1,396.33	1.52
6	Half-normal	~ 1	1,202.46	0.436 ± 0.037	~ distance + plane + glare	194.08	0.545 ± 0.100	1,396.54	1.73
7	Half-normal	~ 1	1,202.46	0.436 ± 0.037	~ distance + plane + size	194.24	0.563 ± 0.096	1,396.69	1.89
8	Half-normal	~ 1	1,202.46	0.436 ± 0.037	~ distance	194.61	0.568 ± 0.092	1,397.07	2.26
9	Half-normal	~ plane + size	1,205.13	0.433 ± 0.039	~ distance + plane	192.35	0.558 ± 0.097	1,397.48	2.67
10	Half-normal	~ plane	1,203.62	0.434 ± 0.037	~ distance + plane + glare	194.08	0.538 ± 0.101	1,397.70	2.89

Table 3. Number of belugas observed by both primary (front) and secondary (rear) observers in both planes combined, and probability of detection at the transect line p(0) based on the best selected mark recapture (double platform) distance models (Table 4).

Parameter	Value
Number seen by primary	70
Number seen by secondary	70
Number seen by both observers	47
Total number of observations	93
p(0) primary observer (± SE)	0.565 ± 0.095 (CV = 0.169)
p(0) secondary observer (± SE)	0.565 ± 0.095 (CV = 0.169)
p(0) combined (± SE)	0.800 ± 0.086 (CV = 0.107)

Table 6. Estimated abundance ($\widehat{N}$) of beluga whales in the Eastern Beaufort Sea population, with standard error, coefficient of variation, lower and upper 95% confidence interval, and degree of freedom, for all offshore strata. Total abundance was corrected for perception bias based on the mark-recapture distance sampling analysis (1/p(0) = 1/0.565 = 1.77) and for bias availability bias (1/P_{laake} = 1/0.516 [SD = 0.115] =1.939).

Stratum	$\widehat{N}$	$se(\widehat{N})$	$CV(\widehat{N})$	Lower $\widehat{N}$	Upper $\widehat{N}$	df
AGE	2,307	678	0.29	1,246	4,271	14.3
BOE	6,050	1,888	0.31	3,174	11,531	16.4
BOW	1,761	582	0.33	831	3,732	7.48
WS	297	67	0.23	154	571	3.49
Total	**10,415**	**2,127**	**0.20**	**6,871**	**15,786**	**25.4**
Total corrected for detection probability	18,433	4,876	0.27	10,794	31,478	25.4
Total corrected for availability bias	35,738	12,364	0.35	17,891	71,387	25.4

Table 7. Survey effort for the NOAA survey in August 2019 for each stratum: area (A) of strata in km^2, distance flown on transect (L) in km, number of transect lines flown (k), area covered by transect (%) calculated as A/Total A, number of belugas observed (n) (number of groups observed), mean group size, and encounter rate (ER) calculated as n/L.

Region	Area (km^2)	Effort (km)	k	Covered Area %	n	Mean size	ER
AGE	19,052	448	5	10.02	65 (45)	1.44	0.145
AGW	35,476	972	9	11.40	241 (189)	1.29	0.248
BOE	72,426	2,879	22	16.23	389 (229)	1.70	0.135
BOW	16,170	651	8	17.45	100 (81)	1.23	0.154
WBI	9,406	303	3	12.89	4 (4)	1.00	0.013
Total	**152,529**	**5,254**	**47**	**14.25**	**799 (548)**	**1.46**	**0.152**

Table 8. Beluga surface abundance estimate by strip transect analysis for the Kugmallit Bay (KB), Shallow Bay (SB) and Mackenzie Bay (MB) stratums for the photographic portion of the survey of the Eastern Beaufort Sea beluga. Columns show data on the area of each strata, the type of aircraft used to cover the area, the number of photos taken within the stratum, the average percentage of overlap between two consecutive photos, the total area covered by photograph (excluding the area that was not investigated because of the presence of glare), the total number of beluga detected in photos (including duplicated belugas located in the overlapping part of the photo), the number of unique beluga detections (excluding the duplicated beluga), the density of belugas within the stratum, the estimated number of belugas at the surface for the entire stratum, the encounter rate (number of beluga per line transect) and the coefficient of variation of the encounter rate (variance estimator 'R2'; Fewster et al. 2009). Lastly, the estimated total number of belugas corrected for availability bias (C_a = 1.56, SD = 0.592) and the associated CV are presented.

Stratum	**Area (km²)**	**Aircraft**	**Date**	**# Photos**	**% Overlap**	**Photo area (km²)**	**Total # beluga in photos**	**# Unique belugas**	**Density (beluga/ km²)**	**# Belugas at surface**	**Encounter rate (CV)**	**Corrected # belugas (CV)**
KB	1,226.05	2	July 23	706	41.7%	195.22	54	38	0.195	239	0.131 (0.525)	373 (0.65)
MB	2,685.95	1 and 2	Aug 2	1,112	33.9%	338.11	60	37	0.109	294	0.071 (0.483)	459 (0.61)
SB	2,036.88	RPAS	Jul 28	876	11.6%	370.24	314	286	0.772	1,574	0.589 (0.300)	2,455 (0.48)
SB	2,036.88	2	Aug 2	889	30.7%	298.45	152	110	0.369	751	0.290 (0.492)	1,171 (0.62)
SB Average	-	-	-	-	-	-	-	-	*0.571*	*1,207*	-	*1,882 (0.61)*
Total	-	-	-	-	-	-	-	-	-	**1,740**	-	**2,714 (0.30)**

Table 9. Comparison of abundance estimate ($\widehat{N}$), 95% confidence interval (CI), and density (number/km^2) for each stratum from two offshore aerial surveys: Fisheries and Oceans Canada (DFO) in 1992[a] and 2019, as well as the encounter rate (ER) (number of beluga sighted/km) of both DFO surveys and the National Oceanic and Atmospheric Administration (NOAA) survey of August 2019. Total abundance corrected for perception bias (1/p(0) = 1.77) in the offshore area and for availability bias (C_a = 2 for the July 1992 survey suggest by Angliss and Outlaw (2005)), C_a = 1.94 (SD = 0.521) for the offshore strata, and C_a = 1.56 (SD = 0.592) for the inshore strata are also presented.

	DFO – July 1992				DFO – July 2019				NOAA – August 2019
Stratum	$\widehat{N}$	**95% CI**[±]	**Density**	**ER**[†]	$\widehat{N}$	**95% CI**	**Density**	**ER**	**ER**
AGE	-	-	-		2,307	1,264–4,271	0.065	0.05	0.145
AGW	2,738	1,526–4,911	0.099	0.052	-	-	-	-	0.248
BOE*	10,572	7,328–15,624	0.204	0.118	6,050	3,174–11,531	0.109	0.089	0.135
BOW	-	-	-	-	1,761	831–3,732	0.12	0.102	0.154
WBI	-	-	-	-	-	-	-	-	0.132
WS	-	-	-	-	297	154–571	0.048	0.037	-
KB	704	394–1,014	1.137	0.92	239	75–765	0.195	-	-
SB	334	208–456	0.314	0.221	1207	402–3,623	0.571	-	-
MB	962	850–1,074	0.507	0.235	294	98–885	0.109	-	-
Total surface uncorrected	**15,307**	**12,305–18,309**	**0.196**	**-**	**12,155**	**8,512–17,357**	**0.103**	**-**	**-**
Total corrected for perception bias	**19,629**	**15,134–24,125**	**0.251**	**-**	**21,073**	**12,575–32,363**	**0.179**	**-**	**-**
Total corrected with for availability bias	***39,258***[±]	***30,268–48,250***	***0.503***	**-**	***38,451***	***20,735–71,304***	***0.327***	**-**	**-**

[a]Data reported in Harwood et al. (1996).
*Results reported in Harwood et al. (1996). West, Middle and East Beaufort Sea were all included within BOE.
[†]Encounter rate calculated from the number of belugas sighted by the primary observer by "kilometers requisite survey conditions" (Table 1 in Harwood et al. 1996).
[±]Only the surface estimate was reported in Harwood et al 1996. A correction factor $C_a = 2$ was suggest by Angliss and Outlaw (2005).

Table 10. Comparison between the 1992 and 2019 surveys by Fisheries and Oceans Canada (DFO) and the 2019 National Oceanic and Atmospheric Administration (NOAA) survey, including coverage (total area of the strata), effort surveyed, number of days flown, and number of days planned for the survey, number of belugas sighted by primary observers, and mean group size, from three offshore aerial surveys.

	DFO – July 1992	**DFO – July 2019**	**NOAA – August 2019**
Coverage (km^2)	74,419	111,506	152,529
Effort (km)	4,130	3,470	5,254
No. of days flown	2	7	17
Survey dates	July 23–25	July 21 – Aug 2	Aug 8–27
No. beluga (primary obs.)	414	278	799
Group size (range)	1.65 (1–12)	1.43 (1–7)	1.46 (1–35)

[a] Data reported in Harwood et al. (1996).

FIGURES

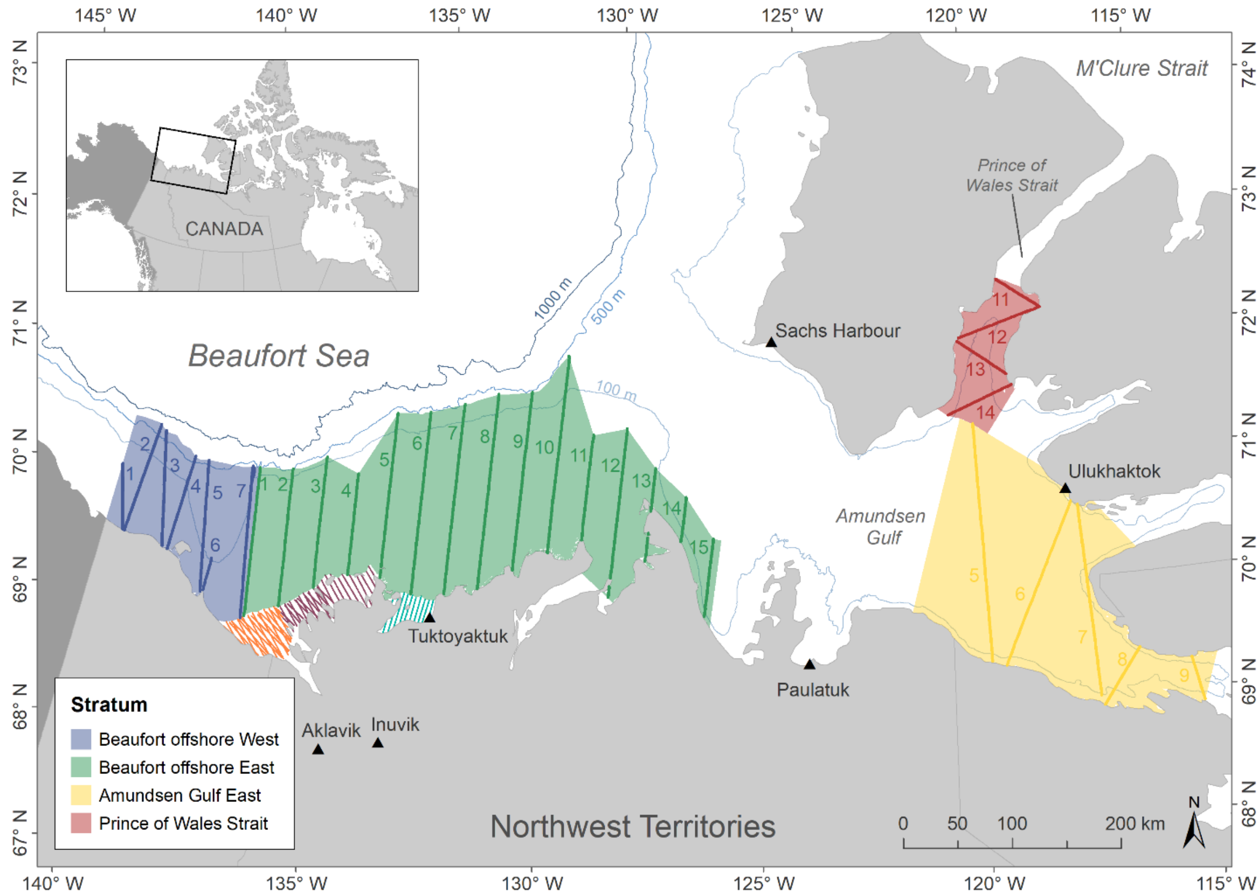

Figure 1. Map of the offshore transects and four main strata flown for the visual survey of the Eastern Beaufort Sea beluga population. Transects were flown on 21, 22 July and 2 August in Beaufort offshore West; 23, 31 July and 2 August for Beaufort offshore East; 27 and 28 July for Amundsen Gulf; and 28 July for Prince of Wales Strait.

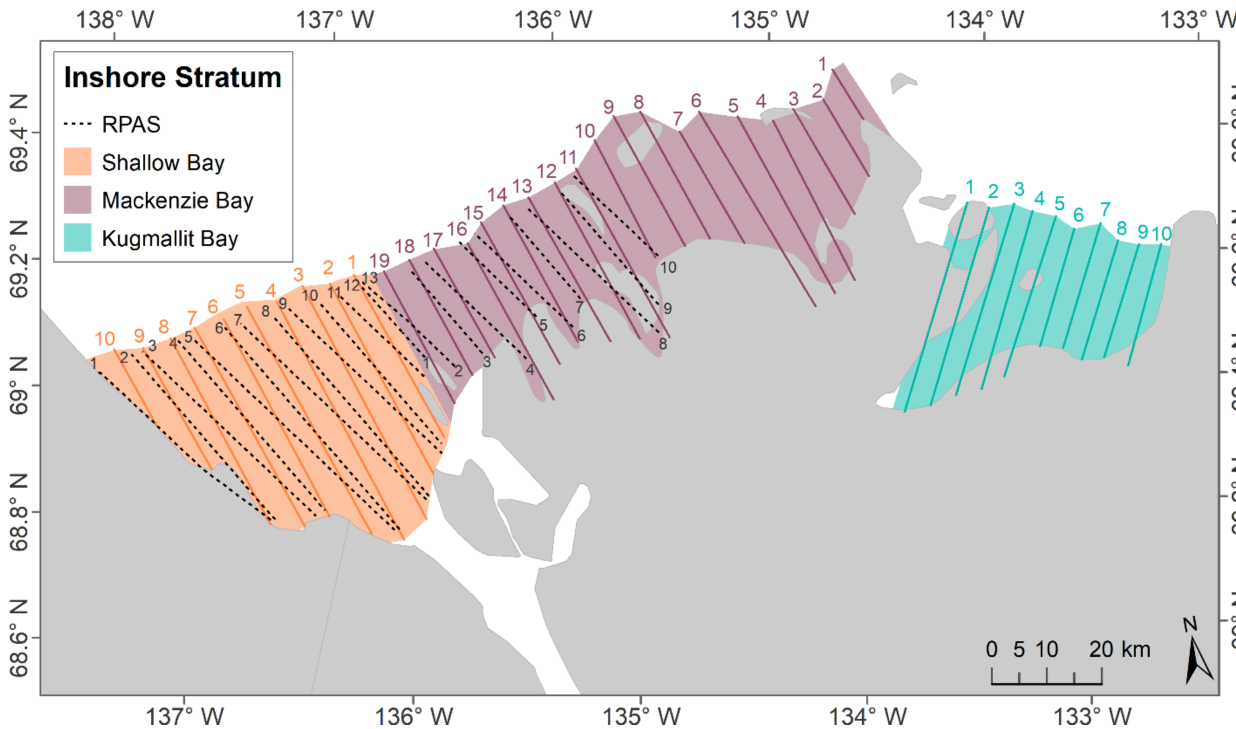

Figure 2. Map of the inshore transects and strata flown by the aircrafts, and by the remotely piloted aircraft system (RPAS) for the photographic survey of the Eastern Beaufort Sea beluga population. Transects were flown on 23 July in Kugmallit Bay, and on 2 August in Shallow Bay and Mackenzie Bay.

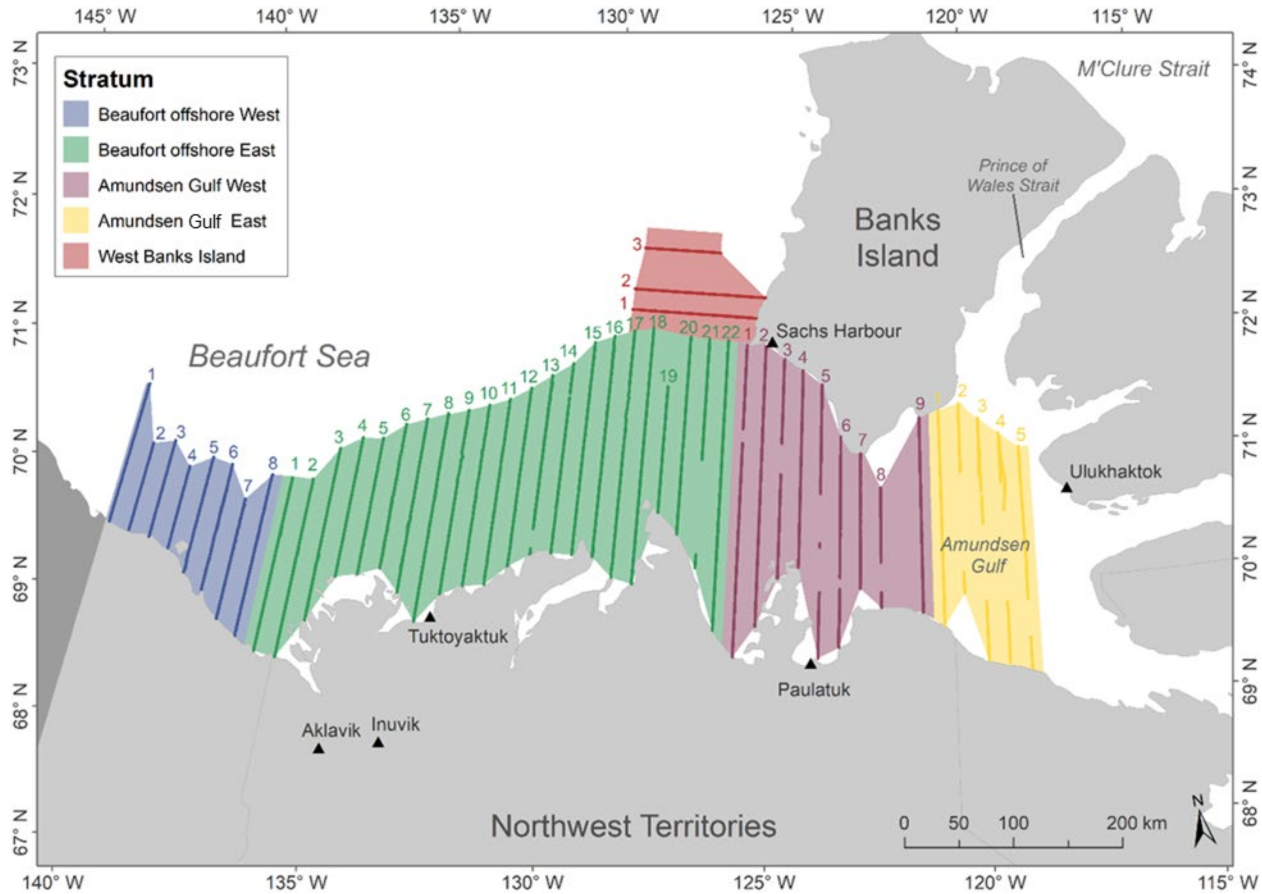

Figure 3. Map of the offshore transects and strata flown between 8 August and 27 August 2019 by the National Oceanic and Atmospheric Administration (NOAA).

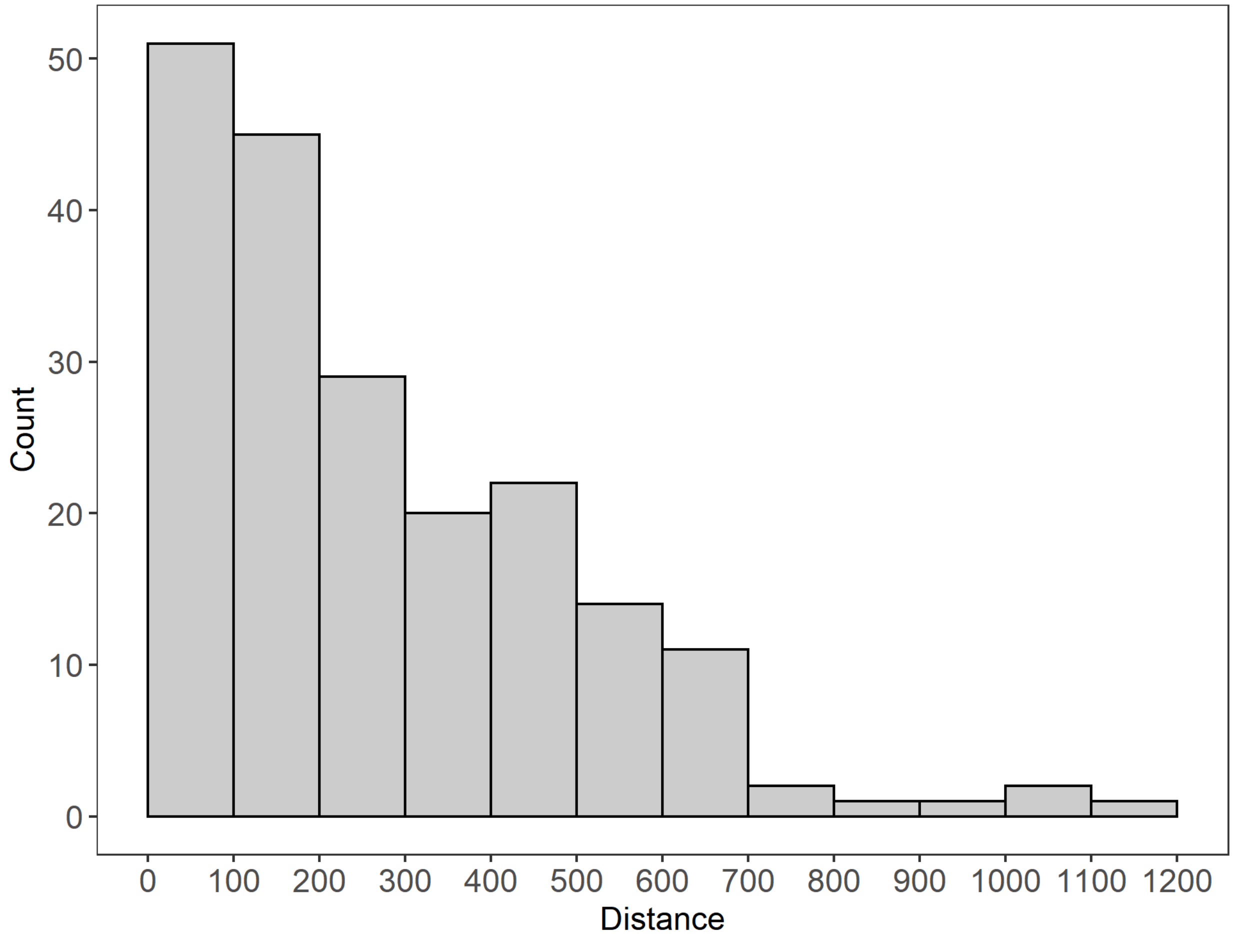

Figure 4. Histogram of perpendicular distances of primary observers only for both planes. Distances considered in the multiple covariate distance sampling analyses.

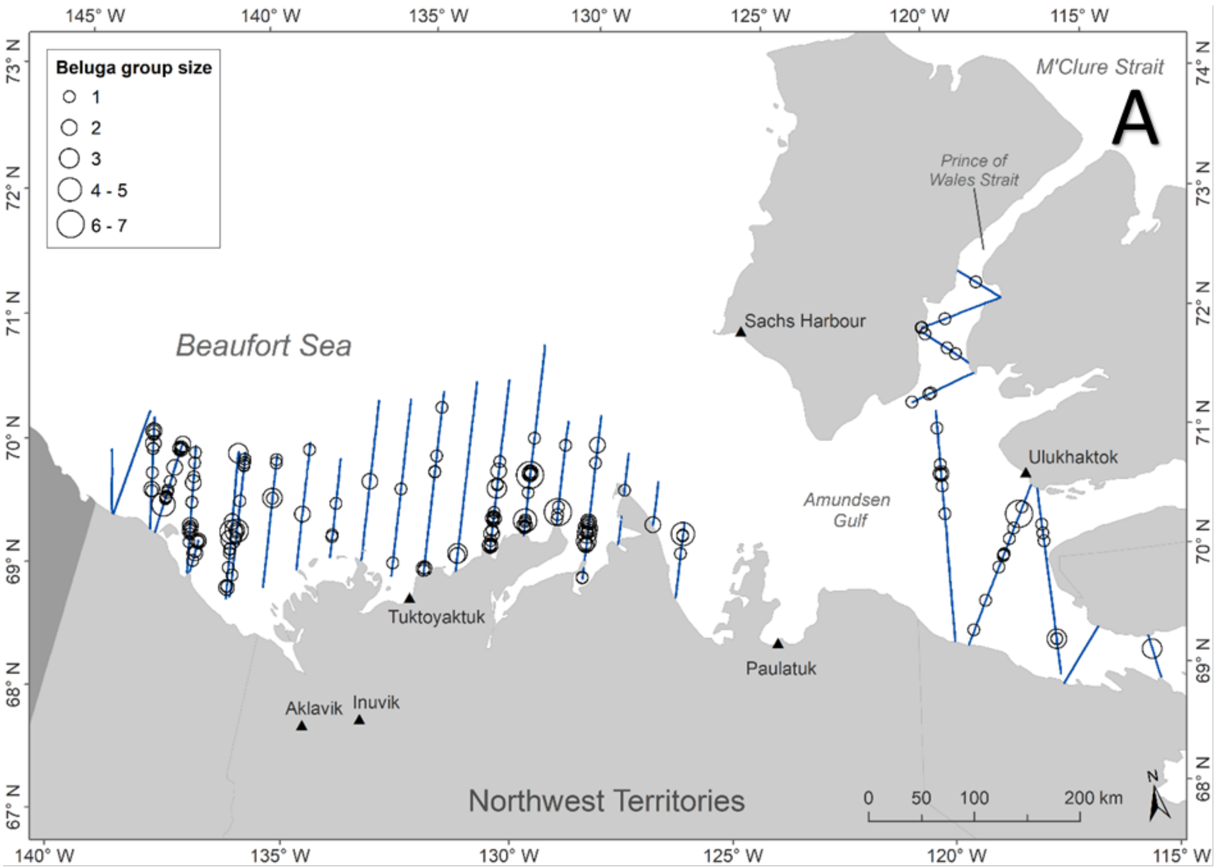

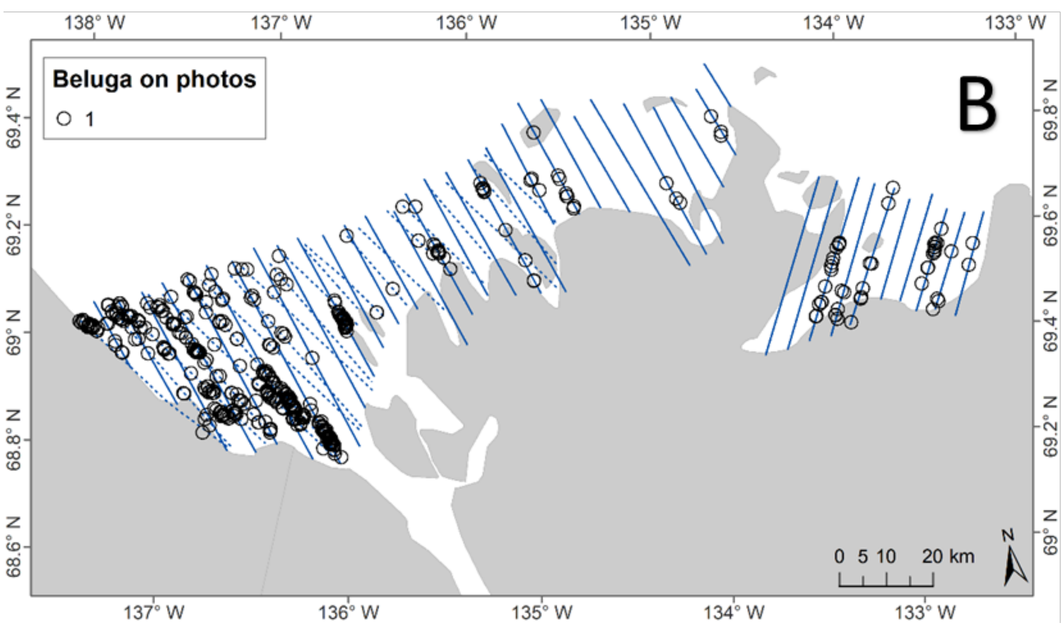

Figure 5. A) Beluga detections offshore (visual survey) and B) inshore (photographic survey) from the 2019 aerial survey conducted by Fisheries and Oceans Canada.

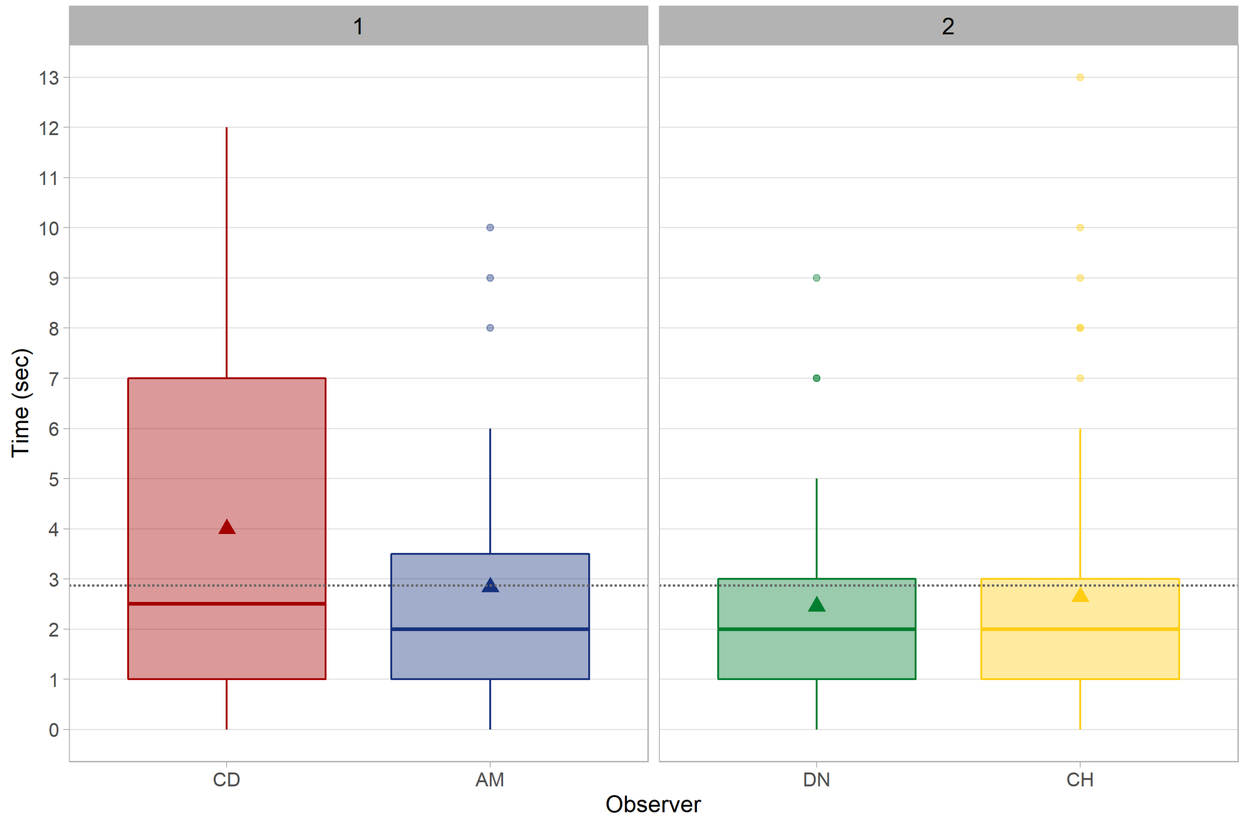

Figure 6. Boxplot of the time difference in seconds between spotting time of a beluga by an observer and the recording of the distance abeam of the aircraft when available (also called time-in-view). The triangle shapes represent the mean time-in-view for each primary observer of plane one (left panel) and plane two (right panel).

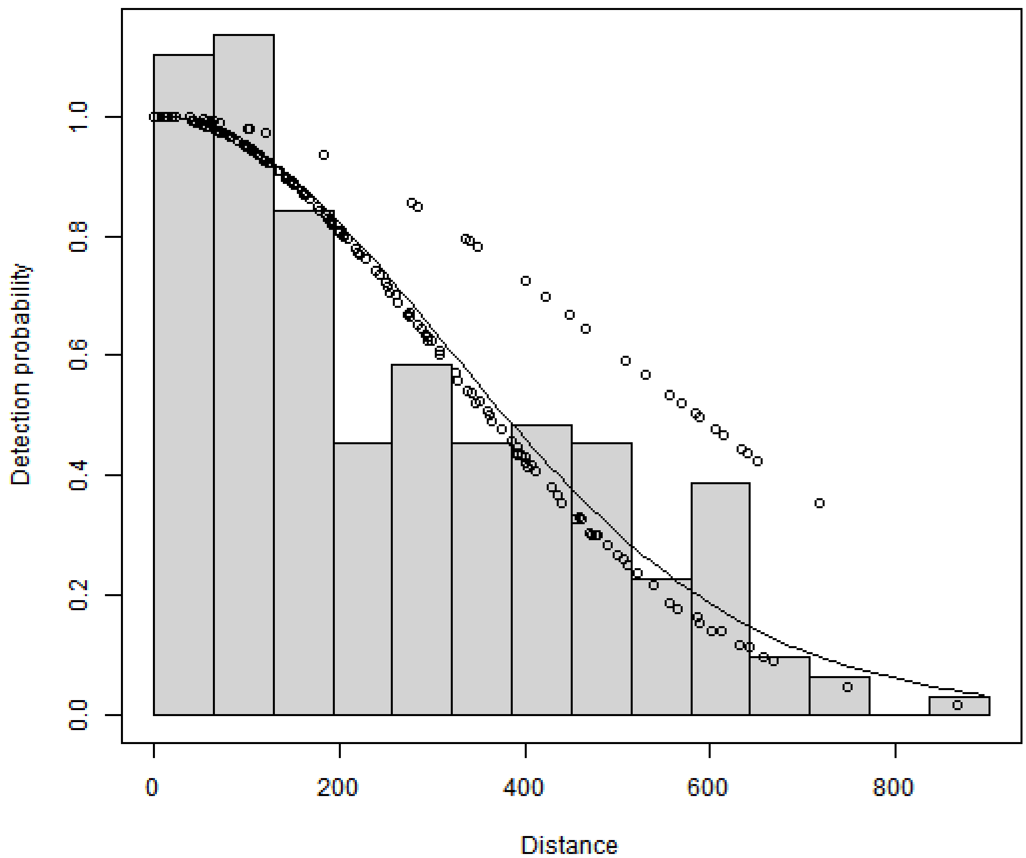

Figure 7. Detection curve (Half-normal key function with glare as covariate) from the multiple covariate distance analyses for the primary observers.

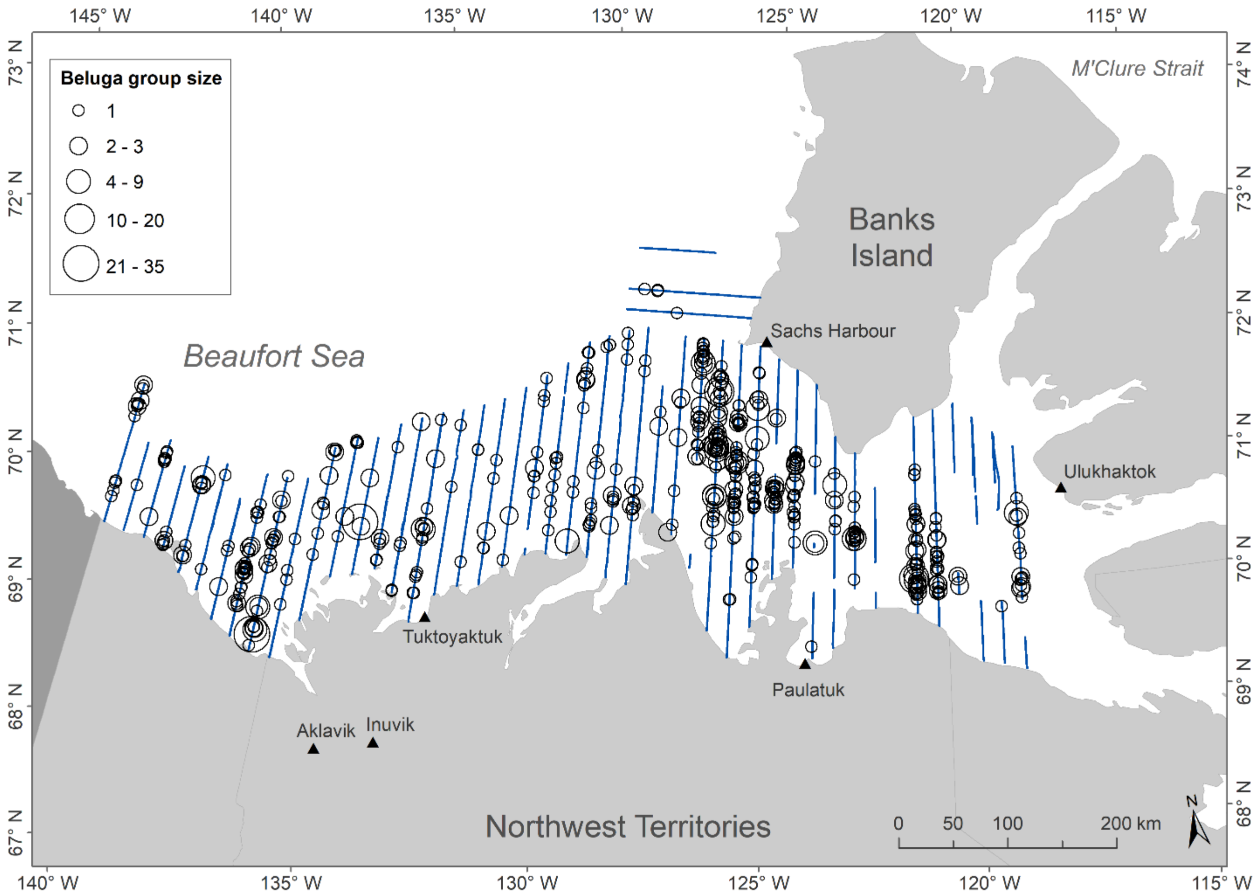

Figure 8. Offshore beluga detections from the 2019 aerial survey conducted by the National Oceanic and Atmospheric Administration between August 8 and August 27, 2019.

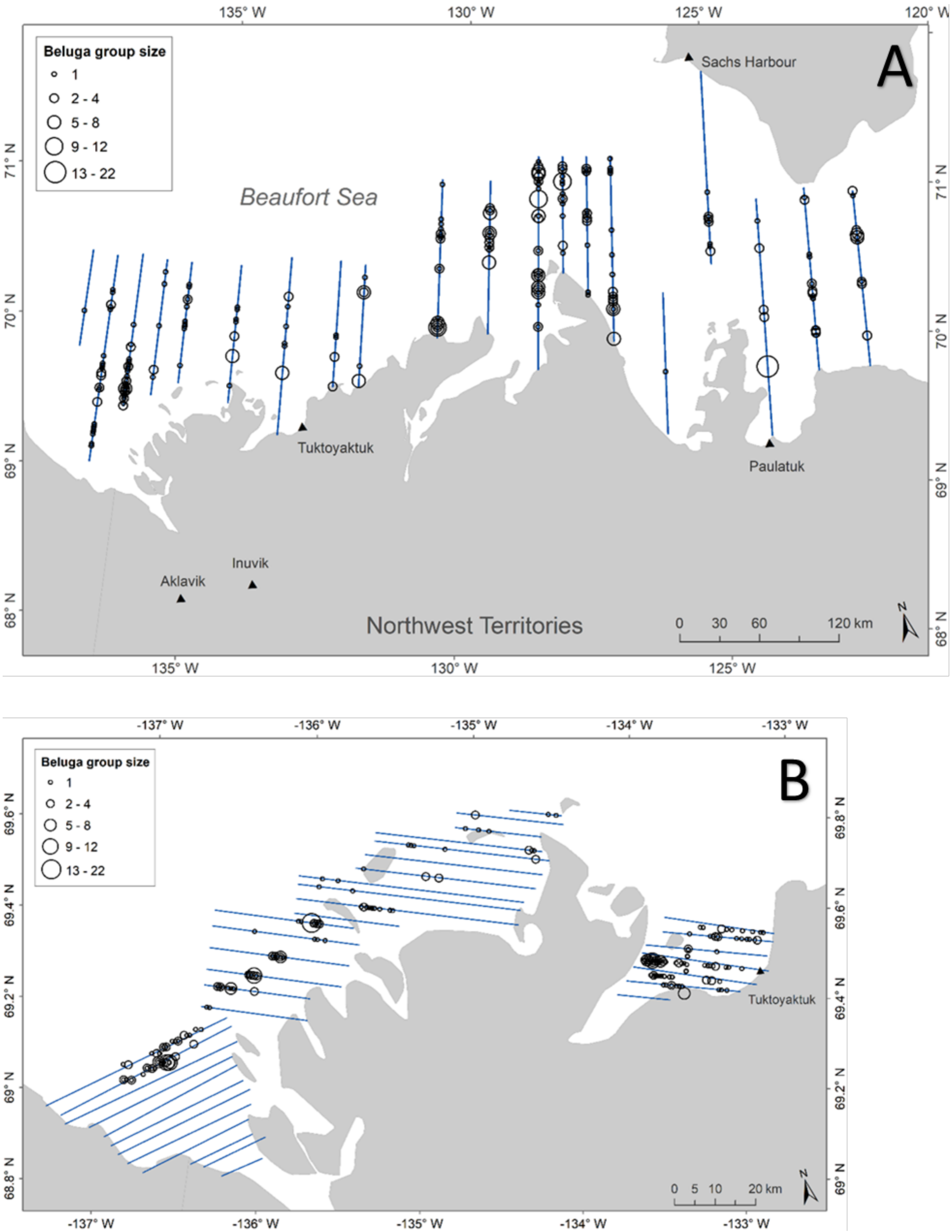

Figure 9. A) Offshore July 24–25, 1992 and B) inshore beluga detections of the July 23, 1992 aerial survey conducted by Fisheries and Oceans Canada. (Harwood and Norton, 1996; Harwood et al. 1996).

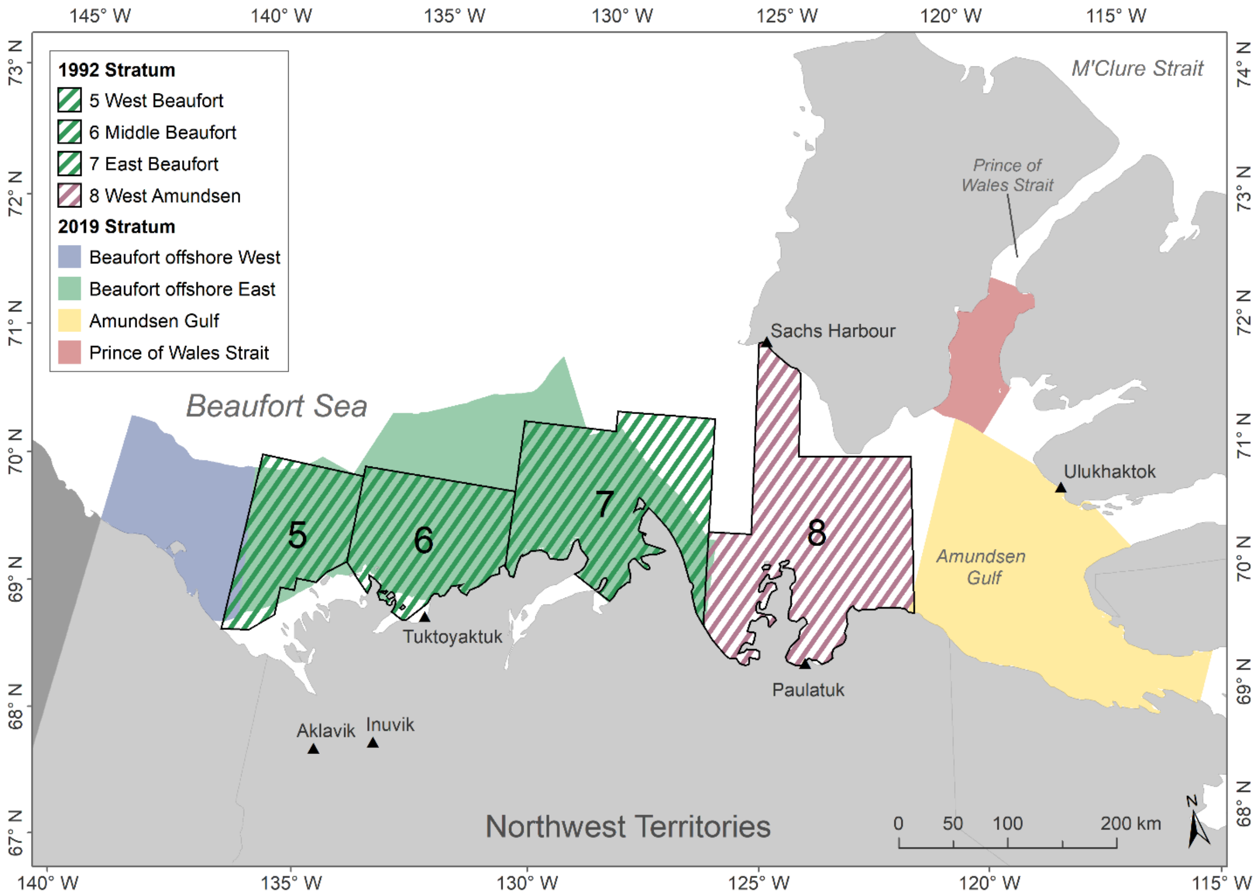

Figure 10. Comparison of the coverage of the 1992 and 2019 aerial surveys conducted by Fisheries and Oceans Canada for the Eastern Beaufort Sea beluga population.

APPENDIX A – DENSITY SURFACE MODELLING

METHOD

Density surface models (DSM) were fitted to estimate the abundance of belugas. Transect lines were split into segments of 2 km in length and 1.8 km width (truncation distance of 900 m), and beluga observations were counted by segment. Using the two-stage approach (Miller et al. 2013), the detection functions from the multiple covariates distances sampling (MCDS) analyses (main document) were first used to correct detectability with respect to the transect flown by both planes. For the second stage, a spatial model was fit to the beluga observations. In addition to the projected longitude and latitude coordinates of the segment centroid (m), five environmental covariates were extracted and tested (Figure A1): sea surface temperature (SST), bathymetry (BATHY), slope (SLOPE), distance to the slope (DIST_SL), and distance to the coastline (DIST_C). The SST was retrieved from the remote sensor MODIS onboard the Aqua satellite and available on NASA's OceanColor Web (https://oceancolor.gsfc.nasa.gov/) at a 4 km resolution for 8-day periods (°C). The bathymetry (m) was retrieved from the 2020 General Bathymetric Chart of the Oceans at $0.00417^{\circ} \times 0.00417^{\circ}$ resolution. The slope was calculated from the bathymetry raster as the difference in degree (°) of the elevation of the four neighboring cells. The distance to the slope (km) was calculated as the distance from the 100 m isobath in the Beaufort shelf. This distance represents the start of the steep slope into the Beaufort Canyon (Weber 1989, Osborne and Forest 2016). Finally, the distance to the coastline (km) was calculated as the distance from the land polygon (Natural Resources Canada, CanVec – Administrative features 5M). Correlation was tested between the covariates with a Spearman’s rank test (see Table A1–A3).

The abundance per segment was modelled with a generalized additive model (Wood 2017). The model was fitted with thin-plate regression splines, using a negative binomial or Tweedie distributions. Duchon splines were also fitted to reduced overfitting at the edge of the survey area (Miller et al. 2013). In addition, the Beaufort offshore West (BOW) and East (BOE) strata were tested separately from the Amundsen Gulf (AG) and Prince of Wales Strait (WS) strata. A “soap film” smoother was fitted for both sections, to smooth over more complicated boundaries (Wood et al. 2008) (the “soap film” was not possible for the whole survey effort as the area was discontinuous). Duchon splines were also tested for both areas. Predicted values were calculated from a 4 km resolution hexagonal grid with covariates extracted at the centroid.

RESULTS

The DSM results were not conclusive. The best model when considering all strata together included bathymetry as covariate, with a Tweedie distribution. However, it only explained 54.30% of the beluga distribution (Table A4) and the prediction map did not match the distribution of beluga sightings (Figure A2). When using Duchon splines with all the strata, full convergence could not be achieved. When BOW and BOE strata were tested separately from the AG and WS strata, the best model also included bathymetry, with the soap film smoother (Table A5). This model only explained 63.75% and produced again a poor representation of the distribution (Figure A3). With Duchon splines, the best model included SST, SLOPE, and DIST_C but only explained 57.32% (Table A5, Figure A4). For the AG and WS strata, none of the models were able to reach full convergence, with thin-plate regression splines, soap films and Duchon splines.

Table A1. Correlation matrix of covariate for all strata together.

	SST	BATHY	SLOPE	DIST_SL
BATHY	0.4	-	-	-
SLOPE	-0.3	-0.6	-	-
DIST_SL	0	-0.1	0.1	-
DIST_C	-0.2	-0.3	0	-0.7

Table A2. Correlation matrix of covariates for the Beaufort offshore West and East strata.

	SST	BATHY	SLOPE	DIST_SL
BATHY	0.5	-	-	-
SLOPE	-0.3	-0.6	-	-
DIST_SL	0.3	0.7	-0.4	-
DIST_C	-0.5	-0.7	0.3	-0.7

Table A3. Correlation matrix of covariates for the Amundsen Gulf and Prince of Wales Strait strata.

	SST	BATHY	SLOPE	DIST_SL
BATHY	-0.5	-	-	-
SLOPE	0.2	0	-	-
DIST_SL	0.5	-0.1	0.4	-
DIST_C	0.4	-0.8	-0.3	-0.2

Table A4. Model results for all strata together, including the distribution (Tweedie (tw) or negative binomial (nb)), the type of smoother for the XY term (thin-plate regression splines (s) or Duchon splines (ds)) with the effective degree of freedom (edf), the covariates included in the model with their edf, the REML values, Akaike information criterion, and the deviation explained (%). Significant terms are identified with an asterisk and the best model is bolded. All models converged.

Distribution	XY smoother (edf)	Covariates (edf)	REML	AIC	Dev. Expl. %
tw	s (15.27)*	SST (1.00) + BATHY (1.00)* + DIST_C (3.40)	263.77	523.84	57.97
tw	s (15.28)*	BATHY (1.00)* + DIST_C (3.40)	264.37	522.40	57.85
tw	s (16.21)*	SST (1.00) + BATHY (1.00)* + DIST_SL (1.00)	265.82	532.41	55.07
tw	s (16.19)*	BATHY (1.00)* + DIST_SL (1.00)	266.39	531.00	54.89
nb	s (15.50)*	SST (1.53) + BATHY (1.00)* + DIST_C (3.16)	267.64	528.74	69.47
tw	s (17.51)*	SST (1.00) + SLOPE (1.36) + DIST_C (2.93)	267.85	527.63	58.09
nb	s (16.53)*	SST (1.25) + BATHY (1.00)* + DIST_SL (1.00)	268.39	533.79	67.40
nb	s (15.73)*	BATHY (1.00)* + DIST_C (3.13)	268.44	526.95	69.23
tw	s (17.86)*	SLOPE (1.32) + DIST_C (2.96)	268.47	526.09	57.96
tw	s (15.91)*	SST (1.00) + SLOPE (1.89) + DIST_SL (4.68)	268.99	530.26	58.11
tw	s (16.38)*	SST (1.00) + BATHY (1.18)*	269.05	532.81	54.45
nb	s (16.64)*	BATHY (1.00)* + DIST_SL (1.00)	269.24	532.17	67.22
tw	**s (16.39)***	**BATHY (1.13)***	**269.58**	**531.36**	**54.30**
tw	s (16.21)*	SLOPE (1.76) + DIST_SL (4.38)	269.75	529.57	57.62
nb	s (15.48)*	SST (1.00) + SLOPE (3.59) + DIST_SL (4.79)	270.45	526.32	71.96
nb	s (17.13)*	SST (1.80) + SLOPE (1.37) + DIST_C (2.75)	271.75	532.59	69.47
nb	s (16.99)*	SST (1.02) + BATHY (1.00)*	271.98	534.11	66.80
nb	s (17.02)*	BATHY (1.00)*	272.78	532.75	66.66

Distribution	XY smoother (edf)	Covariates (edf)	REML	AIC	Dev. Expl. %
nb	s (17.60)*	SLOPE (1.35) + DIST_C (2.68)	272.92	530.65	69.15
tw	s (18.27)*	SST (1.00) + SLOPE (1.50)	272.95	536.61	54.59
tw	s (18.27)*	SLOPE (1.45)	273.53	535.34	54.34
nb	s (18.39)*	SLOPE (1.53) + DIST_SL (1.00)	273.69	537.34	67.04
nb	s (18.18)*	SST (1.53) + SLOPE (3.16)	275.59	536.73	68.36
nb	s (18.24)*	SLOPE (1.34)	276.85	537.29	66.25
tw	s (15.88)*	SST (1.00) + DIST_SL (4.15)	280.96	553.70	55.38
tw	s (17.39)*	SST (1.00) + DIST_C (2.47)	281.32	553.04	55.20
tw	s (16.07)*	DIST_SL (4.00)	281.53	552.46	55.23
tw	s (17.41)*	DIST_C (2.50)	281.79	551.59	55.13
nb	s (15.33)*	SST (1.00) + DIST_SL (4.13)	284.51	556.75	67.16
tw	s (17.95)*	SST (1.00)	284.58	558.24	52.84
tw	s (17.96)*	-	285.05	556.88	52.71
nb	s (15.52)*	DIST_SL (4.17)	285.37	555.11	67.22
nb	s (17.55)*	SST (1.00) + DIST_C (1.79)	286.25	559.13	66.50
nb	s (17.68)*	DIST_C (1.86)	287.01	557.47	66.57
nb	s (17.89)*	SST (1.31)	288.28	561.74	65.14
nb	s (18.13)*	-	289.13	559.77	65.14
tw/nb	ds	Any covariates	Not converging		

Table A5. Model results for BOW and BOE strata with a Tweedie distribution, including the type of smoother for the XY term (soap film (so) or Duchon splines (ds)) with the effective degree of freedom (edf), the covariates included in the model with their edf, the REML values, Akaike information criterion, the deviation explained (%), and the model convergence (Yes/No). Significant terms are identified with an asterisk and the final best model for each smoother type is bolded.

XY smoother (edf)	Covariates (edf)	REML	AIC	Dev. Expl. (%)	Model convergence
so (33.35)*	SST (1.00) + BATHY (1.00)*	247.20	499.88	64.75	Y
so (31.20)*	SST (1.00) + SLOPE (1.00) + DIST_C (2.33)	248.20	510.29	61.98	Y
so (31.04)*	SLOPE (1.00) + DIST_SL (1.00)	248.22	508.03	61.13	Y
so (31.01)*	SLOPE (1.00) + DIST_C (1.36)	248.57	509.93	60.88	Y
so (33.13)*	**BATHY (1)***	**248.96**	**501.64**	**63.75**	**Y**
so (32.54)*	SST (1.00) + SLOPE (1.00)	249.06	509.68	61.47	Y
so (33.11)*	SLOPE (1.00)	249.58	508.81	61.54	Y
so (29.34)*	SST (1.00) + DIST_C (1.86)	263.40	538.39	57.20	Y
so (28.99)*	SST (1.00) + DIST_SL (1.88)	263.51	537.50	57.20	Y
so (29.96)*	DIST_C (1.00)*	263.81	537.27	56.85	Y
so (29.25)*	DIST_SL (2.19)*	263.89	536.36	57.35	Y
so (30.90)*	SST (1.00)	264.63	537.53	57.15	Y
so (31.55)*	-	265.35	536.76	57.25	Y
ds (14.31)*	**SST (1.37e-5)* + SLOPE (1.92e-4)* + DIST_C (7.24)***	**286.39**	**500.09**	**57.32**	**Y**
ds (14.21)*	SLOPE (6.63e-5)* + DIST_C (7.24)*	288.31	499.66	57.26	Y
ds (18.75)*	SST (3.14) + SLOPE (0.46)*	292.49	511.76	59.87	N
ds (21.67)*	SST (1.10e-4)* + BATHY (1.23)	293.13	502.11	59.31	N
ds (19.30)*	SLOPE (1.34) + DIST_SL (1.15)	293.14	507.14	62.94	N
ds (22.16)*	BATHY (1.19e-4)*	295.48	502.33	61.31	N
ds (18.38)*	-	301.61	529.46	53.01	N
ds (13.41)*	SST (1.49e-5)* + DIST_C (7.23)*	304.90	534.02	51.85	Y

XY smoother (edf)	Covariates (edf)	REML	AIC	Dev. Expl. (%)	Model convergence
ds (21.59)*	SST (1.07e-4)* + DIST_SL (3.35)	305.95	519.98	59.65	N
ds (3.53)*	DIST_C (3.05)*	306.66	573.94	29.02	N
ds (7.10)*	SLOPE (2.00)	314.77	572.14	37.47	N
ds (6.87)*	SST (3.40)	323.62	589.77	37.27	N
ds (6.89)*	DIST_SL (3.68)*	644.32	1,152.73	39.25	N

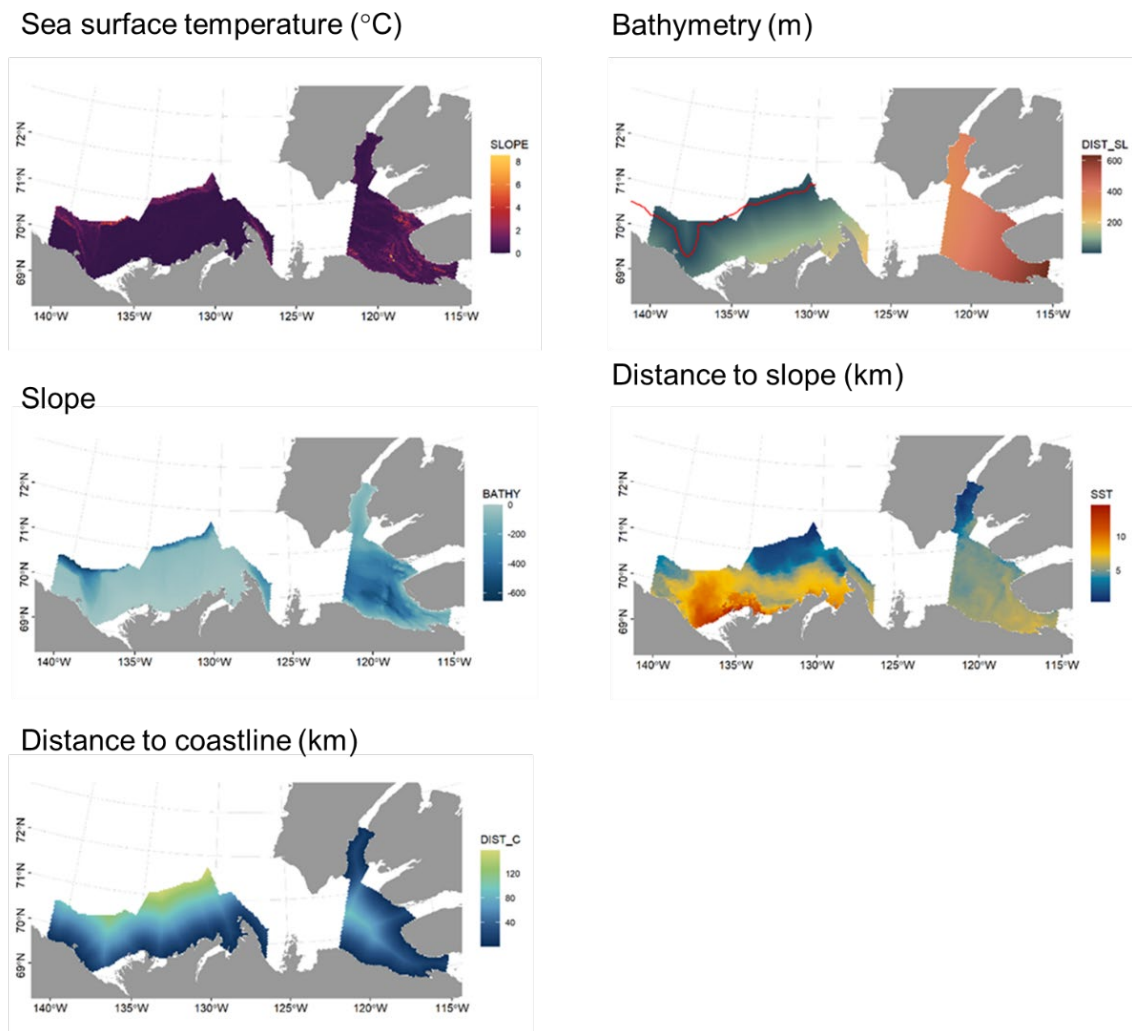

Figure A1. Maps of the environmental covariates included in the density surface models of the distribution of beluga sightings.

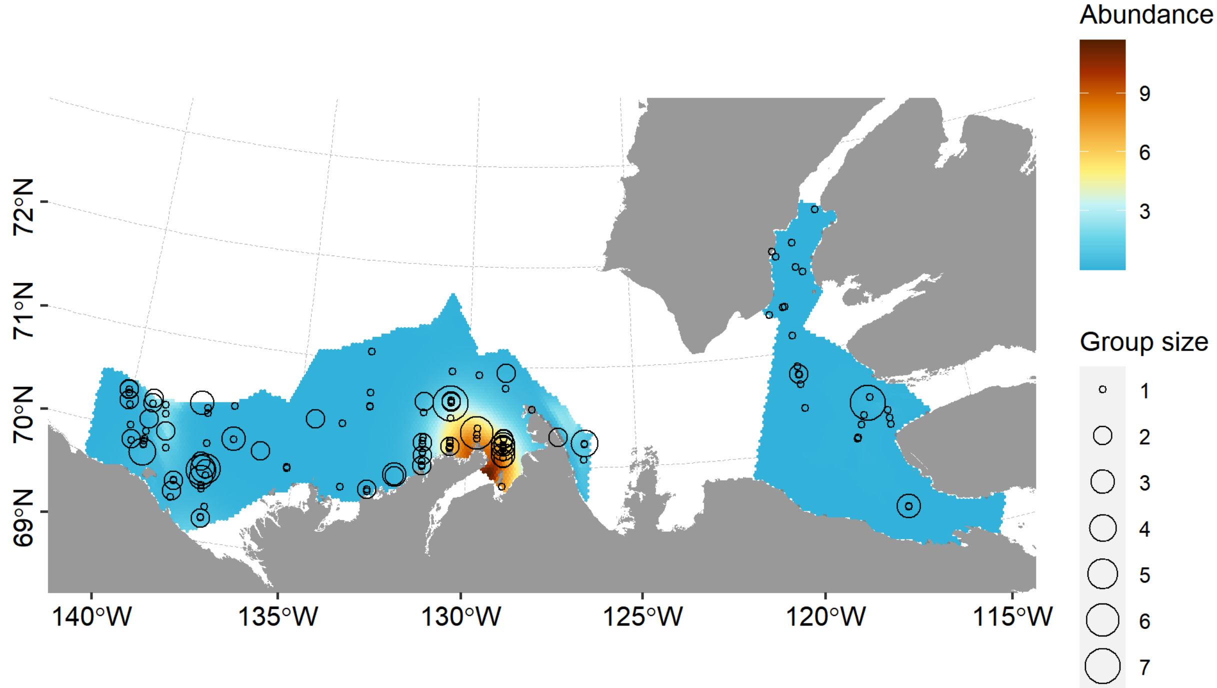

Figure A2. Prediction map of the beluga abundance with the density surface model for all strata (XY with "thin-plate regression splines" smoother and bathymetry as covariate). Abundance estimated = 3,706 belugas.

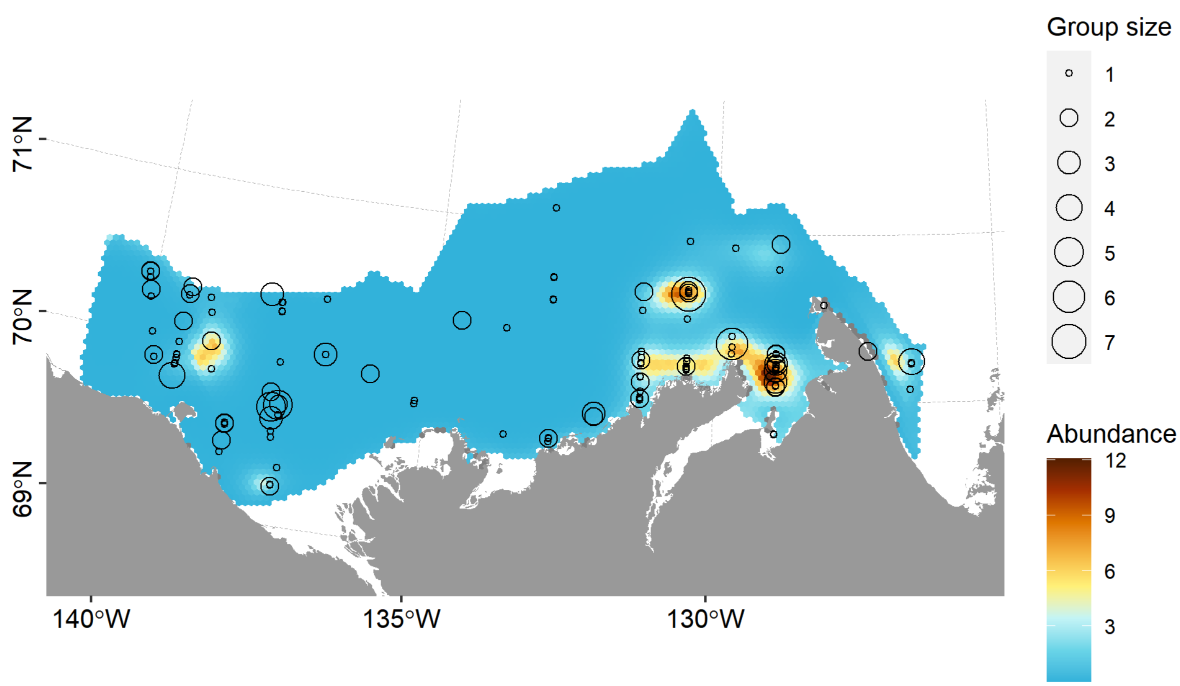

Figure A3. Prediction map of the beluga abundance with the density surface model for BOW and BOE only (XY with "soap film" smoother and bathymetry as covariate). Abundance estimated = 2,498 belugas.

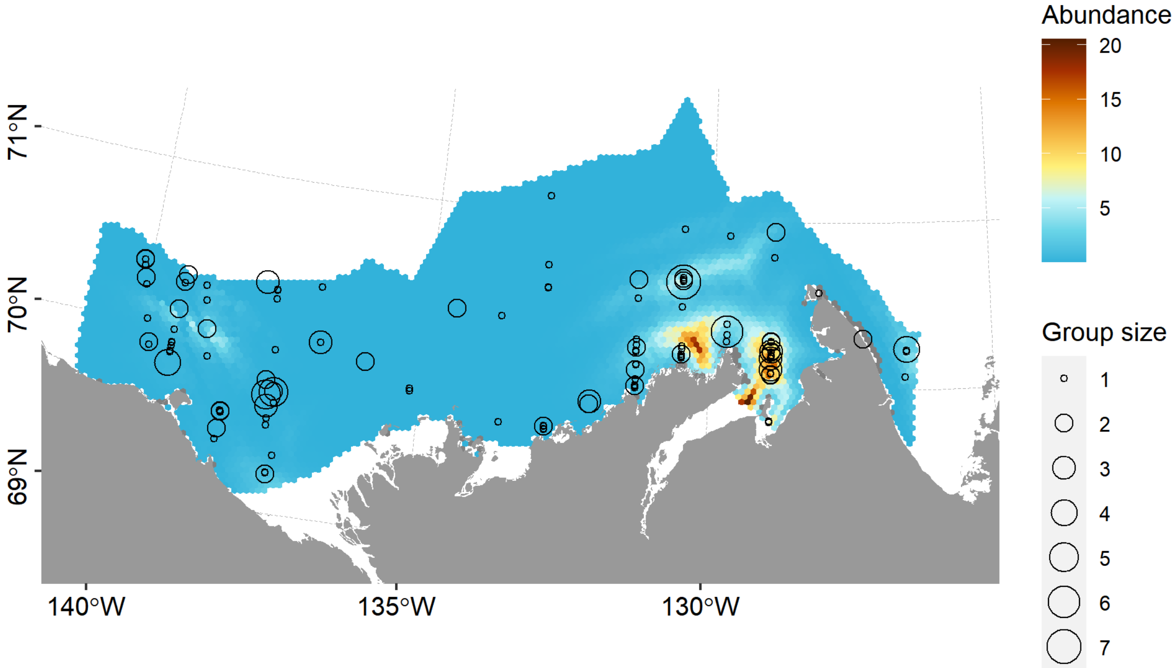

Figure A4. Prediction map of the beluga abundance with the density surface model for BOW and BOE only (XY with "Duchon splines" smoother and sea surface temperature, slope, and distance to coastline as covariates). Abundance estimated = 3,240 belugas.

APPENDIX B – FIGURES

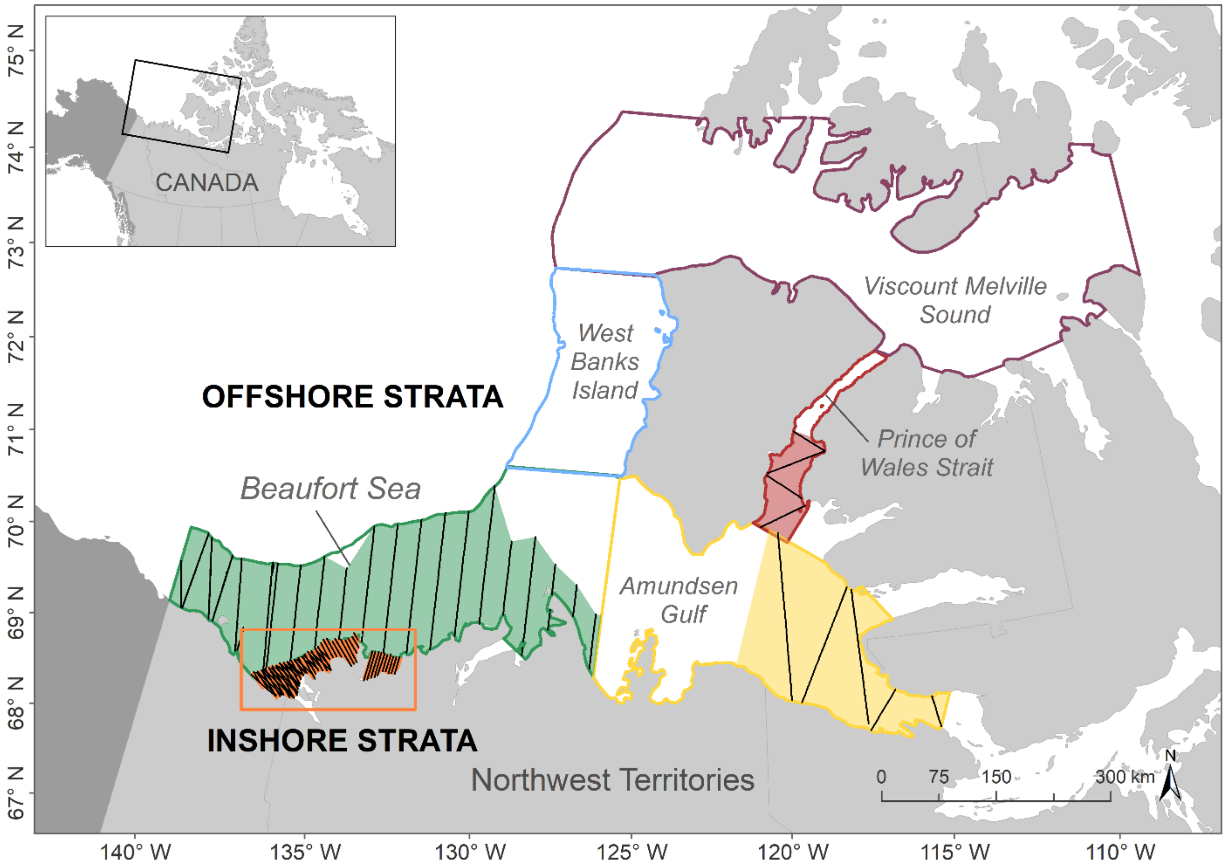

Figure B1. Map of the planned (colored contour) and realized (shaded polygons) strata and transects flown (black lines) from the 2019 aerial survey of the Eastern Beaufort Sea beluga population.